**The EMBO Journal (2012) 31,** 1062–1079 | © 2012 European Molecular Biology Organization | All Rights Reserved 0261-4189/12
www.embojournal.org

THE EMBO JOURNAL

# A novel pathway combining calreticulin exposure and ATP secretion in immunogenic cancer cell death

**Abhishek D Garg[1], Dmitri V Krysko[2,3], Tom Verfaillie[1], Agnieszka Kaczmarek[2,3], Gabriela B Ferreira[4], Thierry Marysael[5], Noemi Rubio[1], Malgorzata Firczuk[6,7], Chantal Mathieu[4], Anton JM Roebroek[8], Wim Annaert[9], Jakub Golab[6,7], Peter de Witte[5], Peter Vandenabeele[2,3] and Patrizia Agostinis[1,*]**

[1]Cell Death Research and Therapy Unit, Department of Cellular and Molecular Medicine KU Leuven, KU Leuven, Leuven, Belgium, [2]Molecular Signaling and Cell Death Unit, Department for Molecular Biomedical Research, VIB, Ghent, Belgium, [3]Department of Biomedical Molecular Biology, Ghent University, Ghent, Belgium, [4]Laboratory for Experimental Medicine and Endocrinology (LEGENDO), Department of Clinical and Experimental Medicine, KU Leuven, Leuven, Belgium, [5]Laboratory for Pharmaceutical Biology, Department of Pharmaceutical and Pharmacological Sciences, KU Leuven, Leuven, Belgium, [6]Department of Immunology, Centre of Biostructure Research, Medical University of Warsaw, Warsaw, Poland, [7]Department 3, Institute of Physical Chemistry, Polish Academy of Sciences, Warsaw, Poland, [8]Experimental Mouse Genetics, Department of Human Genetics, KU Leuven, Leuven, Belgium and [9]Laboratory for Membrane Trafficking, Department of Human Genetics, KU Leuven and VIB-Center for the Biology of Disease, Leuven, Belgium

**Surface-exposed calreticulin (ecto-CRT) and secreted ATP are crucial damage-associated molecular patterns (DAMPs) for immunogenic apoptosis. Inducers of immunogenic apoptosis rely on an endoplasmic reticulum (ER)-based (reactive oxygen species (ROS)-regulated) pathway for ecto-CRT induction, but the ATP secretion pathway is unknown. We found that after photodynamic therapy (PDT), which generates ROS-mediated ER stress, dying cancer cells undergo immunogenic apoptosis characterized by phenotypic maturation ($CD80^{high}$, $CD83^{high}$, $CD86^{high}$, $MHC\text{-}II^{high}$) and functional stimulation ($NO^{high}$, $IL\text{-}10^{absent}$, $IL\text{-}1\beta^{high}$) of dendritic cells as well as induction of a protective antitumour immune response. Intriguingly, early after PDT the cancer cells displayed ecto-CRT and secreted ATP before exhibiting biochemical signatures of apoptosis, through overlapping PERK-orchestrated pathways that require a functional secretory pathway and phosphoinositide 3-kinase (PI3K)-mediated plasma membrane/extracellular trafficking. Interestingly, eIF2α phosphorylation and caspase-8 signalling are dispensable for this ecto-CRT exposure. We also identified LRP1/CD91 as the surface docking site for ecto-CRT and found that depletion of PERK, PI3K p110α and LRP1 but not caspase-8 reduced the immunogenicity of the cancer cells. These results unravel a novel PERK-dependent subroutine for the early and simultaneous emission of two critical DAMPs following ROS-mediated ER stress.**

*The EMBO Journal* (2012) **31,** 1062–1079. doi:10.1038/emboj.2011.497; Published online 17 January 2012
*Subject Categories*: signal transduction; molecular biology of disease
*Keywords*: calreticulin; cancer; DAMPs; immunogenic apoptosis; photodynamic therapy

## Introduction

Current anticancer regimens mediate killing of tumour cells mainly by activating apoptosis, an immunosuppressive or even tolerogenic cell death process. However, it has recently emerged that a selected class of cytotoxic agents (e.g., anthracyclines) can cause tumour cells to undergo an immunogenic form of apoptosis and these dying tumour cells can induce an effective antitumour immune response (Locher *et al*, 2010). Immunogenic apoptosis of cancer cells displays the main biochemical hallmarks of 'tolerogenic' apoptosis: phosphatidylserine exposure, caspase activation, and mitochondrial depolarization. However, this type of cell death also seems to have two other important properties: (1) surface exposure or secretion of critical 'immunogenic signals' that fall in the category of damage-associated molecular patterns (DAMPs; Zitvogel *et al*, 2010a) and (2) the ability to elicit a protective immune response against tumour cells (Obeid *et al*, 2007; Green *et al*, 2009; Garg *et al*, 2010b; Zitvogel *et al*, 2010b).

Several DAMPs have recently been identified as crucial for immunogenic apoptosis. These include surface calreticulin (ecto-CRT), surface HSP90 (ecto-HSP90), and secreted ATP (Spisek *et al*, 2007; Kepp *et al*, 2009). Ecto-CRT has been shown to act primarily as an 'eat me' signal (Gardai *et al*, 2005), presumably essential for priming the innate immune system, since depletion of CRT by siRNA knockdown averts the immunogenicity of cancer cell death (Obeid *et al*, 2007). Similarly, bortezomib-induced ecto-HSP90 exposure is crucial for immunogenic death of tumour cells and their subsequent contact with dendritic cells (DCs; Spisek *et al*, 2007). On the other hand, secreted ATP acts either as a 'find me' signal or as an activator of the NLRP3 inflammasome (Elliott *et al*, 2009; Ghiringhelli *et al*, 2009). However, while the signalling pathways governing surface exposure of CRT have been delineated to some extent (Panaretakis *et al*, 2009), insufficient information exists on the molecular pathway behind ATP secretion. Finally, immunogenic apoptosis is sometimes associated with disappearance of certain surface-associated molecules, for example CD47, which are referred to as 'do not eat me' signals (Chao *et al*, 2010).

*Corresponding author. Department of Cellular and Molecular Medicine, Faculty of Medicine, University of Leuven (KU Leuven), Campus Gasthuisberg O&N1, Herestraat 49, Box 901, 3000 Leuven, Belgium. Tel.: +32 16 345715; Fax: +32 16 345995;
E-mail: patrizia.agostinis@med.kuleuven.be

**Received: 5 April 2011; accepted: 21 December 2011; published online: 17 January 2012**

 

One common feature of all immunogenic apoptosis-inducing stimuli so far identified is induction of endoplasmic reticulum (ER) stress (Panaretakis *et al*, 2009; Garg *et al*, 2010b; Zitvogel *et al*, 2010b). Importantly, in the case of ecto-CRT triggered by anthracyclines, both ER stress and reactive oxygen species (ROS) production have been found to be mandatory (Panaretakis *et al*, 2009). However, anthracyclines suffer from dose-limiting side effects (Minotti *et al*, 2004; Vergely *et al*, 2007). Moreover, ROS production is neither a primary effect of anthracyclines nor predominantly ER directed, which makes the anthracycline-induced 'ROS-based' ER stress less effective and secondary in nature (Minotti *et al*, 2004; Vergely *et al*, 2007).

Thus, we envisaged that one way of improving the immunogenicity of dying cancer cells is by using a therapeutic approach that can generate strong ROS-dependent ER stress as a primary effect (Garg *et al*, 2011). We hypothesized that photodynamic therapy (PDT; Agostinis *et al*, 2011) might fit the criterion of primary ER-directed ROS production. PDT can induce oxidative stress at certain subcellular sites by activating organelle-associated photosensitizers (Castano *et al*, 2006; Buytaert *et al*, 2007). Once excited by visible light and in the presence of oxygen, photosensitizers can generate organelle-localized ROS that can cause lethal damage to the cells (Agostinis *et al*, 2002). Additionally, this ROS-based anticancer therapy can also cause 'emission' of DAMPs and activate the host immune system (Korbelik *et al*, 2005; Garg *et al*, 2010a).

To test this hypothesis, we used the ER-associated photosensitizer, hypericin. When it is activated by light, it causes a ROS-mediated loss-of-function of SERCA2 with consequent disruption of ER-$Ca^{2+}$ homeostasis, followed by BAX/BAK-based mitochondrial apoptosis (Buytaert *et al*, 2006). This photo-oxidative ER stress (phox-ER stress) is accompanied by transcriptional upregulation of components of the unfolded protein response (UPR) and by changes in the expression of various genes coding for immunomodulatory proteins (Buytaert *et al*, 2008; Garg *et al*, 2010a).

We report here that phox-ER stress induces immunogenic apoptosis in treated cancer cells. Early after phox-ER stress and largely preceding phosphatidylserine externalization, cancer cells mobilize CRT at the surface and secrete ATP through an overlapping PERK- and phosphoinositide 3-kinase (PI3K)-mediated mechanism, which is dissociated from caspase signalling. Intriguingly, we found that LRP1 is required for the docking of ecto-CRT.

## Results

### *Phox-ER stress causes cancer cells to undergo immunogenic apoptosis*

At the outset, we decided to investigate whether cancer cells dying in response to phox-ER stress (Hyp-PDT based; unless otherwise mentioned) can activate human immature DCs (hu-iDCs). We used phox-ER stress (Supplementary Figure S1) mediated apoptosis-inducing conditions reported in our previous studies (Hendrickx *et al*, 2003; Buytaert *et al*, 2006) generating ~87% of cell death of the human bladder carcinoma T24 cells within 24 h (Supplementary Figure S2). T24 cells subjected to Hyp-PDT underwent phagocytic interactions with hu-iDCs (Figure 1A). They were also phagocytosed by Mf4/4 phagocytes preferentially over untreated T24 cells (Supplementary Figure S3). Moreover, these Hyp-PDT-treated dying T24 cells induced phenotypic maturation of hu-iDCs, as indicated by surface upregulation of MHC class II (HLA-DR) and co-stimulatory CD80, CD83 and CD86 molecules (Figure 1B; Supplementary Figure S4A and B). The significant surface expression of these molecules was similar to that induced by lipopolysaccharide (LPS), a known pathogen-associated molecular pattern (PAMP) (Figure 1B; Supplementary Figure S4A and B). In contrast, freeze-thawed T24 cells undergoing accidental necrosis (AN) did not strongly stimulate DC maturation (Figure 1B; Supplementary Figure S4A and B). These findings rule out the possibility that AN might be responsible for the increased DC maturation seen against phox-ER stressed cells.

To get further insight into the functional status of DCs, we evaluated the pattern of certain cytokines including the generation of nitric oxide (NO) as a marker for respiratory burst (Stafford *et al*, 2002). We compared DCs exposed to Hyp-PDT-treated T24 cells with those exposed to LPS or T24 cells dying following AN. We found that hu-iDCs exposed to Hyp-PDT-treated cancer cells displayed a distinguished pattern of functional activation characterized by $NO^{high}$, IL-$10^{absent}$ (Figure 1C and D). This was clearly different from that induced by accidental necrotic cells ($NO^{high}$, IL-$10^{high}$) or by LPS ($NO^{low}$, IL-$10^{low}$) (Figure 1C and D). Interestingly, LPS and especially accidental necrotic cells stimulated the production of IL-10 (Figure 1D), whereas Hyp-PDT-treated cells failed to stimulate the production of this immunosuppressive cytokine (Kim *et al*, 2006; Zitvogel *et al*, 2006) by hu-iDCs.

To investigate the ability of cancer cells undergoing phox-ER stress to activate the adaptive immune system, we carried out *in-vivo* experiments in immunocompetent BALB/c mice. Before initiating the *in-vivo* experiments, we optimized the mouse colon carcinoma CT26 cell line for Hyp-PDT-induced apoptosis (Supplementary Figure S5) and ER stress (Supplementary Figure S1). As observed previously in other cells (Hendrickx *et al*, 2003; Buytaert *et al*, 2006), hypericin colocalized strongly with ER Tracker (Supplementary Figure S5A) and upon light irradiation induced not only appreciable cell killing (Supplementary Figure S5B) but also the main hallmarks of apoptosis, including caspase-3 and PARP cleavage (Supplementary Figure S5C). Furthermore, the CT26 cells exposed to Hyp-PDT were preferentially phagocytosed over untreated CT26 cells by murine JAWSII DCs (Supplementary Figure S6). Then, in the *in-vivo* study, we immunized BALB/c mice with Hyp-PDT-treated dying/dead CT26 cells. As positive and negative controls for immunogenic cell death, respectively, we used CT26 cells treated with the anthracycline, mitoxantrone (MTX) or tunicamycin (TN, an inhibitor of N-linked glycosylation) (Obeid *et al*, 2007). The immunized mice were then rechallenged with live CT26 tumour cells. Protection against tumour growth at the rechallenge site was interpreted as a sign of successful priming of the adaptive immune system (Figure 1E). Mice immunized with CT26 cells treated with MTX or Hyp-PDT showed robust signs of activation of the adaptive immune system: both procedures strongly prevented the tumour growth seen in the non-immunized mice. By contrast, most of the mice immunized with tunicamycin-treated CT26 cells experienced tumour growth after rechallenge (Figure 1E), which confirms the poor

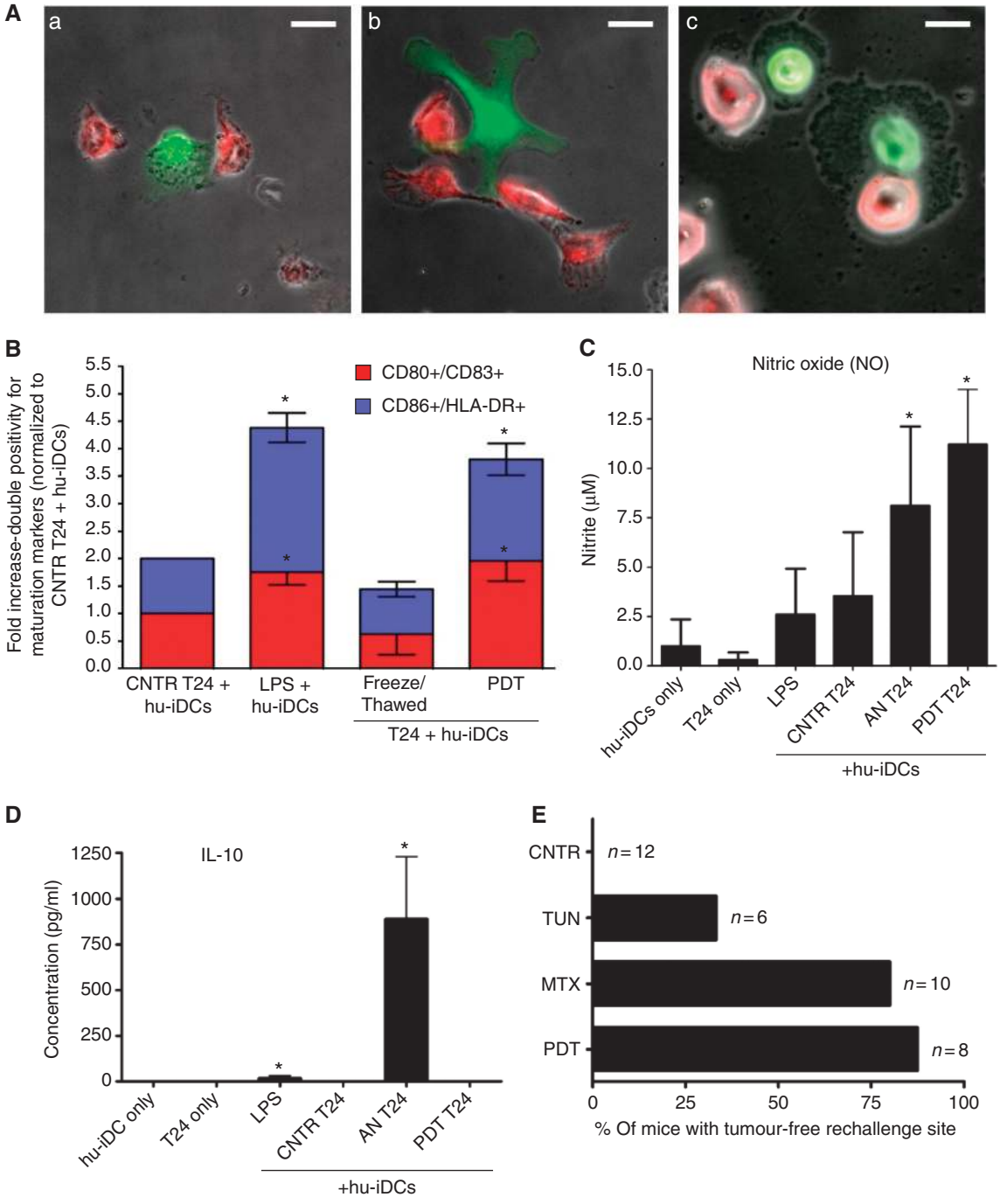


**Figure 1** Tumour cells dying under phox-ER stress conditions induce DC maturation and activate the adaptive immune system. (**A**) *In-vitro* phagocytosis of T24 cells treated with Hyp-PDT (red) by human immature dendritic cells (hu-iDCs) (green). The confocal fluorescence images show various phagocytic interactions between dying T24 cells and hu-iDCs, such as tethering (a), initiation of engulfment by extending the pseudopodia (b), and final stages of engulfment (c); scale bar = 20 μm. (**B**) Human DC maturation analysis. T24 cells were left untreated (CNTR), freeze/thawed (accidental necrosis = AN), or treated with a high PDT dose. They were then co-incubated with hu-iDCs. As a positive control, hu-iDCs were stimulated with LPS for 24 h. After co-incubation, the cells were immunostained in two separate groups for CD80/CD83 positivity and CD86/HLA-DR positivity and scored by FACS analysis. Data have been normalized to the 'CNTR T24 + hu-iDCs' values. Fold change values are means of two independent experiments (two replicate determinations in each) ± s.e.m. (*$P<0.05$, versus 'CNTR T24 + hu-iDCs'). (**C**, **D**) Cytokine and respiratory burst patterns exhibited by human DCs. The T24-hu-iDC co-incubation conditioned media obtained during the experiments detailed in (**B**) were recuperated followed by analysis for concentrations of nitrite (solubilized form of nitric oxide or NO) (**C**), and IL-10 (**D**). Absolute concentrations are the means of two independent experiments (four replicate determinations in each) ± s.d. (*$P<0.05$ versus hu-iDC only). (**E**) Priming of adaptive immune system by dead/dying CT26 cells. Following immunization with PBS (CNTR) or with CT26 cells treated with tunicamycin (TUN), mitoxantrone (MTX) and the highest PDT dose, the mice were rechallenged with live CT26 tumour cells. Subsequently, the percentage of mice with tumour-free rechallenge site was determined (*n* represents the number of mice).

immunogenic properties of cancer cell death induced by this ER stress agent (Obeid *et al*, 2007). These data suggest that apoptotic cancer cells dying from phox-ER stress induced by Hyp-PDT activate the immune system, which is one of the important properties of immunogenic apoptosis.

 

### *Cancer cells exposed to phox-ER stress surface expose or secrete/release immunogenic DAMPs*

We next analysed the surface exposure/release of CRT, secreted ATP and extracellular heat-shock proteins (i.e., HSP90 and HSP70) following phox-ER stress using three different Hyp-PDT doses—low, medium, and high PDT. Moreover, because of the reported effects of anthracyclines, MTX, and doxorubicin (DOXO) on immunogenic cell death (Obeid *et al*, 2007), we used them throughout the study for comparison.

Ecto-CRT surface exposure, detected by immunofluorescence staining of T24 cells treated with Hyp-PDT or MTX, showed the characteristic surface 'patches' reported previously (Gardai *et al*, 2005; Obeid *et al*, 2007; Figure 2A). Cell surface biotinylation followed by immunoblot analysis of the isolated plasma membrane proteins derived from T24 cancer cells treated with Hyp-PDT revealed that phox-ER stress (Supplementary Figure S1) induced enhanced surface exposure of CRT (Figure 2B). This ecto-CRT preceded apoptosis-associated phosphatidylserine exposure (Supplementary Figure S2) under plasma membrane non-permeabilizing conditions (Figure 2C). On-cell western assay (Gonzalez-Gronow *et al*, 2007) confirmed these results (Supplementary Figure S7). In general, Hyp-PDT was observed to be superior to DOXO and MTX (Figure 2D and E), in terms of mobilizing CRT to the surface of cancer cells. Moreover, ecto-CRT was detectable as early as 30 min after Hyp-PDT and increased with time (Figure 2E). The 30-min threshold is much earlier than reported for anthracyclines (Obeid *et al*, 2007). This induction of ecto-CRT by Hyp-PDT was diminished in the presence of the $^1O_2$ quencher L-histidine, thus revealing its ROS dependence (Buytaert *et al*, 2006; Supplementary Figure S8A). In contrast to anthracycline-induced ecto-CRT exposure (Panaretakis *et al*, 2008), ecto-CRT exposure following Hyp-PDT was not accompanied by co-translocation of ERp57 to the surface (Figure 2B).

Likewise ecto-HSP90, certain ER proteins, such as calnexin (CNX), PERK and BiP were also undetectable on the surface of the cells under the same conditions that efficiently mobilized ecto-CRT (Supplementary Figure S8B). In addition, several other ER proteins have been reported to undergo translocation to the plasma membrane (Zai *et al*, 1999; Korbelik *et al*, 2005; Zhang *et al*, 2010). Therefore, we used cell surface biotinylation combined with immunoblotting to screen for surface-translocated proteins containing the KDEL 'ER retrieval' signal sequence, in wild-type (WT) and $CRT^{-/-}$ MEFs. Ecto-CRT (~63 kDa) was the only protein with the KDEL sequence recognizable on the surface of Hyp-PDT-treated cells (Figure 2F). No KDEL-containing proteins were found in the plasma membrane fraction of cells lacking CRT (Figure 2F). On the other hand, KDEL sequences of ER resident proteins, such as GRP94, GRP78, ERp72 (ER resident protein 72), and PDI, were identifiable by their molecular weights in the intracellular protein fractions of WT and $CRT^{-/-}$ cells (Figure 2F). Overall, these results indicate that phox-ER stress does not lead to a general surface scrambling of ER proteins (luminal or membrane associated) but rather to a selective and rapid surface exposure of CRT in pre-apoptotic conditions.

We next asked whether photo-oxidative stress mediated by other photosensitizers known to localize to other subcellular sites in addition to the ER were equally capable of surface-exposing CRT. To this end, we used photofrin (PF-PDT), a photosensitizer used in the clinic and known to induce phox-ER stress (Szokalska *et al*, 2009). Interestingly, while phox-ER stress mediated by Hyp-PDT strongly induced ecto-CRT, it was not so for PF-PDT (Supplementary Figure S8C) under similar apoptosis-inducing conditions as reported previously (Szokalska *et al*, 2009). This difference between Hyp-PDT and PF-PDT in ecto-CRT induction might be due to the more pronounced ER localization of hypericin when compared with photofrin (Buytaert *et al*, 2007; Szokalska *et al*, 2009; Luo *et al*, 2010). These data further underline the importance of a robust ER-directed oxidative stress in inducing ecto-CRT.

Next, we addressed the possibility that apart from induction of ecto-CRT, Hyp-PDT-treated T24 cancer cells can secrete ATP into the extracellular environment. Analysis of the conditioned media showed that T24 cancer cells treated with Hyp-PDT secreted ATP (Figure 3A) under non-permeabilizing plasma membrane conditions (Figure 2C). Secretion of ATP preceded apoptosis-associated phosphatidylserine exposure (Supplementary Figure S2) and downregulation of the 'do not eat me' signal CD47 (Supplementary Figure S8D). Interestingly, at least at medium Hyp-PDT dose, the corresponding intracellular ATP content rose considerably in the pre-apoptotic stages (Figure 3B).

It has been shown that extracellular ATP can activate NLRP3-dependent IL-1β production by DCs (Ghiringhelli *et al*, 2009). Hence, we quantified IL-1β secretion in the co-incubation conditioned media used in the DC maturation analysis experiments. We found that the hu-iDCs released significant amounts of IL-1β when exposed to accidental necrotic T24 cells or those treated with Hyp-PDT, and in greater amounts than that released against untreated T24 cells or after LPS treatment (Figure 3C). This further substantiates the possibility of inducing immunogenic cancer cell death by phox-ER stress. Moreover, we also detected passive extracellular release of CRT, HSP90, and HSP70 (Figure 3D) in the conditioned media of late apoptotic cancer cells.

These data together indicate that phox-ER stress induced by Hyp-PDT in cancer cells causes an early induction of ecto-CRT and active secretion of ATP in stressed cells, followed by late apoptotic passive release of HSPs such as HSP70 and HSP90. Thus, from the data presented in this and the previous section, we conclude that phox-ER stress can induce immunogenic apoptosis in cancer cells.

### *Ecto-CRT induction and ATP secretion follow overlapping trails consisting of a secretory pathway and PI3K-dependent plasma membrane/extracellular trafficking*

DAMPs observed in the current study reached the extracellular space actively, thereby implying a possible role for active transport mechanisms like the secretory pathway in their emission. For investigating this plausibility, we used several well-established small molecule inhibitors that affect the (early biosynthetic and/or distal) secretory pathway.

Inhibition of microtubule-dependent retrograde transport with nocodazole did not affect ecto-CRT induction (Supplementary Figure S9A). However, inhibition of ER-to-

Golgi transport (i.e., early biosynthetic pathway) with brefeldin A (BFA) reduced ecto-CRT induction in cancer cells treated with anthracyclines or Hyp-PDT (Figure 4A and B). Furthermore, the translocation of CRT was found to be actin dependent because latrunculin B, an actin inhibitor, reduced ecto-CRT induction in treated cancer cells (Supplementary Figure S9B). Intriguingly, BFA also reduced the ability of cancer cells to secrete ATP after Hyp-PDT treatment (Figure 4C). The intracellular levels of ATP were not affected significantly by the presence of BFA (data not shown). This observation also points to ER and Golgi as possible sources for the ATP actively secreted after Hyp-PDT. Thus, these data

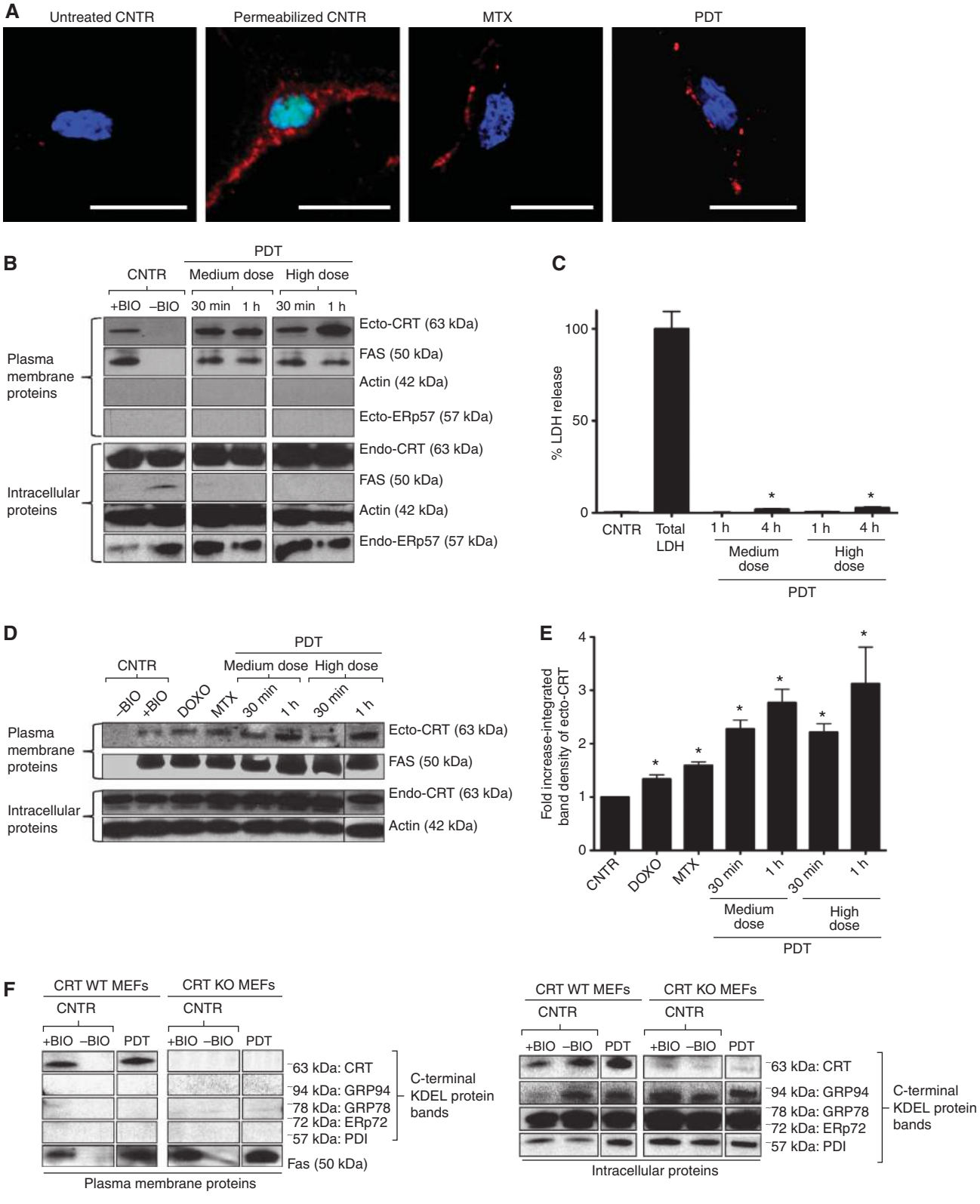

suggest that both CRT and ATP follow ER-to-Golgi transport pathway to reach the plasma membrane or be secreted.

In the distal secretory pathway, PI3Ks have been reported to modulate the plasma membrane trafficking and mediate exocytotic/secretory processes which are wortmannin sensitive (Campos-Toimil *et al*, 2002; Safaei *et al*, 2005; Abe *et al*, 2009; Low *et al*, 2010). Inhibition of secretion/plasma membrane trafficking by wortmannin (Wilson and Guild, 2001; Cousin *et al*, 2003; Laurino *et al*, 2005) reduced ecto-CRT in cancer cells treated with anthracyclines or Hyp-PDT (Figure 4D and E). In fact, Hyp-PDT-induced secretion of ATP was also found to be sensitive to wortmannin-based inhibition (Figure 4F), whereas wortmannin did not affect the intracellular ATP levels (data not shown). Since, wortmannin tends to exhibit a high affinity for the p110α domain of the PI3K protein (Campos-Toimil *et al*, 2002; Yuan and Cantley, 2008) we used a small hairpin RNA (shRNA) to stably deplete the PI3K p110α protein in CT26 cancer cells (Supplementary Figure S9C) in order to confirm the specific involvement of PI3Ks in plasma membrane/extracellular trafficking of CRT and ATP. Knockdown of PI3K p110α significantly attenuated ecto-CRT induction, after both anthracyclines and Hyp-PDT treatment (Figure 4G), as well as ATP secretion after Hyp-PDT treatment (Figure 4H) in cancer cells.

Thus, we conclude that in response to phox-ER stress, CRT and ATP reach the extracellular space by following overlapping molecular pathways consisting of the classical secretory pathway and PI3K-dependent (wortmannin inhibitable) plasma membrane/extracellular trafficking.

### *Cells subjected to phox-ER stress display ecto-CRT and secrete ATP through a common molecular pathway requiring PERK*

ER stress-associated molecular mechanisms behind pre-apoptotic ecto-CRT induction, which we will refer to as the 'canonical CRT pathway', were recently scrutinized for anthracycline-based immunogenic cell death. The pathways involved were mainly governed by PERK-mediated S51 eIF2α phosphorylation, ER-proximal caspase-8 activation, BAX/BAK and ER-$Ca^{2+}$ depletion (Panaretakis *et al*, 2009). Therefore, we evaluated the relevance of these molecular components in the induction of ecto-CRT by phox-ER stress and used anthracyclines (MTX or DOXO) as a reference for 'canonical CRT pathway' inducers.

Hyp-PDT was capable of inducing early eIF2α phosphorylation and late CHOP induction, which indicates that functional activation of the UPR (Supplementary Figure S1) was taking place (Buytaert *et al*, 2008). Cells lacking PERK were incapable of exposing ecto-CRT after Hyp-PDT or anthracyclines treatment (Figure 5A). Moreover, shRNA-based stable knockdown of PERK in CT26 cancer cells (Supplementary Figure S10A) also reduced ecto-CRT (Figure 5B). These results highlight the crucial role of PERK in mediating ecto-CRT induction. In agreement with previous work (Panaretakis *et al*, 2009), cells in which the WT eIF2α was replaced heterozygously with a non-phosphorylable S51A mutant failed to induce ecto-CRT in response to anthracyclines treatment, but Hyp-PDT-induced ecto-CRT was not affected (Figure 5C). Moreover, we observed that cells lacking PERK (Figure 5D) as well as cancer cells with depleted PERK (Figure 5E) failed to secrete ATP following Hyp-PDT treatment (whereas in both cases, the intracellular ATP content was not affected (data not shown)). Interestingly, it has been recently reported that PERK might play a crucial role in proper secretory pathway functioning (Gupta *et al*, 2010; Teske *et al*, 2011). Since, following phox-ER stress, both ecto-CRT (Figure 4B) and secreted ATP (Figure 4C) were reduced by defects in the secretory pathway we wondered whether ablation of PERK affected the cell's ability to maintain a proper secretory protein load. Interestingly, we observed that following Hyp-PDT, while PERK competent cells were able to efficiently modulate their total extracellular secretory protein content (Supplementary Figure S10B and C) cells lacking PERK (Supplementary Figure S10B) or cancer cells with depleted PERK (Supplementary Figure S10C) exhibited difficulties in maintaining corresponding levels of total extracellular secretory protein content. Thus, under phox-ER stress, PERK might help in proper maintenance of extracellular secretory protein load.

Next, to address the involvement of ER-proximal caspases in CRT surface translocation, we used zVAD-fmk, a pan-caspase inhibitor. We found that zVAD-fmk strongly suppressed anthracycline-induced ecto-CRT in cancer cells (Figure 6A), but it did not affect ecto-CRT induction following Hyp-PDT (Figure 6A). Similar effects were also observed in HeLa cells (Figure 6B). These observations suggest that ecto-CRT induced by phox-ER stress is caspase independent. In line with these findings, ecto-CRT induction by Hyp-PDT was not diminished in cells overexpressing the cytokine response

**Figure 2** Phox-ER-stressed cancer cells expose calreticulin on the surface (ecto-CRT). (**A**) Immunofluorescence analysis of ecto-CRT. T24 cells were treated with MTX (1 μM for 4 h) and a high PDT dose (recovered 1 h post PDT) or left untreated (CNTR). Alternatively, some cells were saponin permeabilized. This was followed by staining with Sytox Green (exclusion dye), fixation, and immunostaining for CRT and counterstaining with DAPI; scale bar = 20 μm. (**B**) Surface biotinylation analysis of ecto-CRT following phox-ER stress. T24 cells were treated with indicated doses of PDT. They were recovered at the indicated intervals after PDT treatment. Surface proteins were biotinylated followed by immunoblotting. In (**B**), (**D**), and (**F**), '+BIO' indicates controls exposed to buffer with biotin and '−BIO' indicates controls exposed to buffer without biotin (negative control). (**C**) Plasma membrane permeabilization kinetics following phox-ER stress. T24 cells were treated with PDT and the resulting conditioned media derived at the indicated times post-PDT were analysed for the presence of cytosolic LDH. Total LDH content was determined following Triton-based permeabilization of cells. Data are presented as percent LDH release; values are means of five replicate determinations ± s.d. (*$P<0.05$, versus CNTR). (**D**) Phox-ER stress induces more ecto-CRT than anthracyclines. T24 cells were treated with PDT, DOXO (25 μM for 4 h), and MTX (1 μM for 4 h). They were recovered at the indicated intervals after PDT treatment. Surface proteins were biotinylated as described for (**B**). (**E**) Integrated band densitometric analysis of ecto-CRT. T24 cells were treated with DOXO (25 μM for 4 h), MTX (1 μM for 4 h), and PDT (dose and recovery time points are indicated); and surface proteins were resolved as detailed in (**B**). Following this, the ecto-CRT protein bands were quantified for the integrated band density *via* Image J software. Data have been normalized to the CNTR values. Fold change values are means of three independent determinations ± s.e.m. (*$P<0.05$, versus CNTR). (**F**) Surface biotinylation analysis for KDEL sequence detection following phox-ER stress. CRT WT and KO MEFs were treated with a low PDT dose and surface biotinylated as mentioned in (**B**). Immunoblotting was done to detect the C-terminal KDEL sequence of various ER proteins (expected molecular weights are indicated).

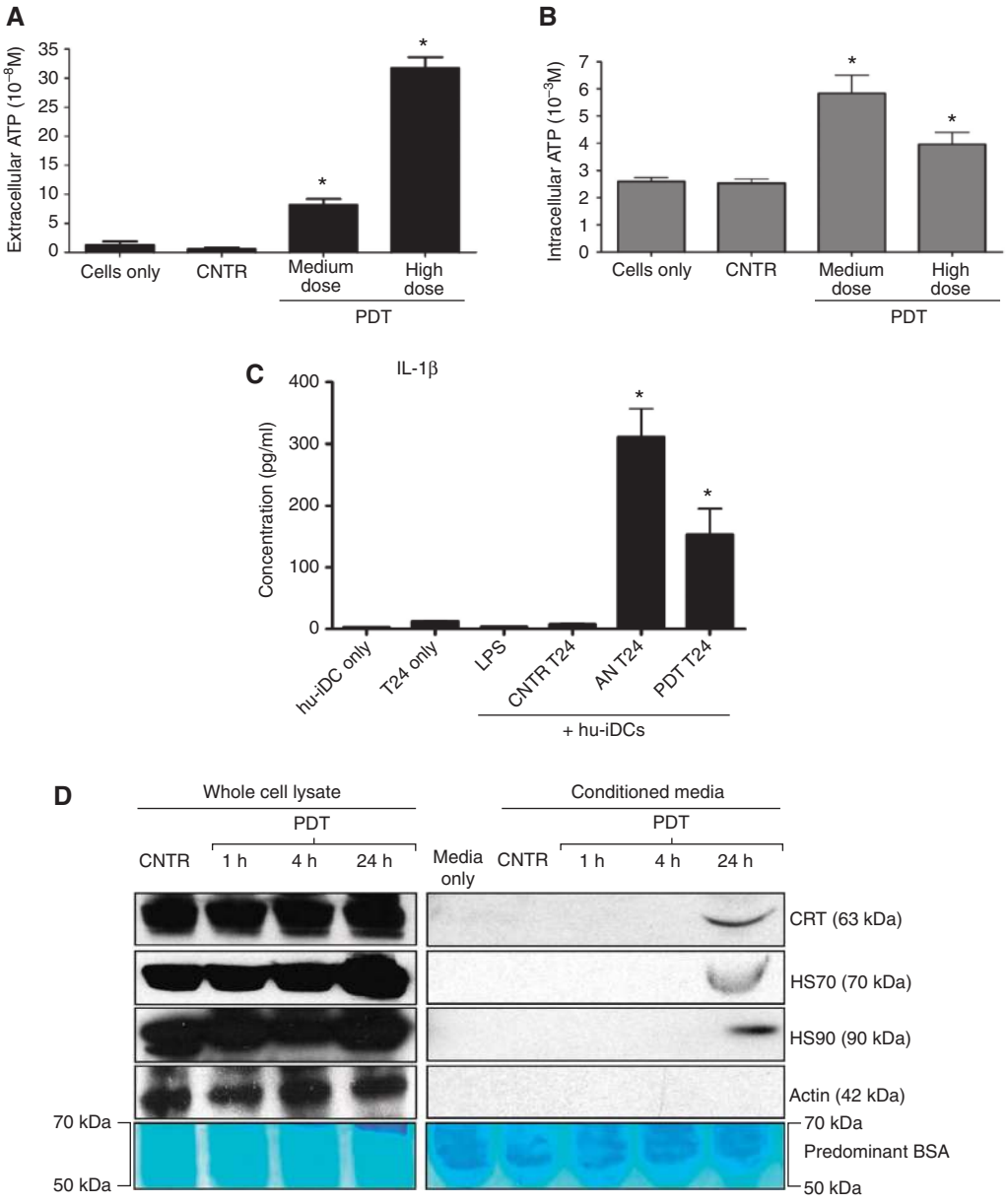


**Figure 3** Cancer cells exposed to phox-ER stress actively secrete ATP, passively release HSP70, HSP90, CRT, and induce IL-1β production in DCs. (**A**, **B**) ATP secretion following phox-ER stress. T24 cells were treated with PDT or left untreated (CNTR), and the conditioned media derived from these cells (1 h post PDT in serum-free media) were analysed for the presence of ATP (**A**). Simultaneously, the corresponding cells were permeabilization with saponin (1 h post PDT) followed by determination of ATP content in the lysate (**B**). Absolute concentrations are mean values of six replicate determinations ± s.d. (*$P<0.05$, versus CNTR). (**C**) Cancer cells subjected to phox-ER stress stimulate IL-1β production in hu-iDCs. T24 cells were treated to undergo accidental necrosis (AN), or treated with a high PDT dose (recovered 24 h post PDT), and then co-incubated with hu-iDCs for 24 h. Simultaneously hu-iDCs were stimulated with LPS. After co-incubation, the co-incubation conditioned media (CCM) were analysed for the presence of IL-1β. Cytokine concentrations (in pg/ml) are means of two independent experiments (four replicate determinations in each) ± s.e.m. (*$P<0.05$, versus CNTR T24). (**D**) Passive release of HSP70, HSP90, and CRT by dying T24 cells. T24 cells were treated with PDT and recovered at the indicated times. The conditioned media (CM) derived from these cells were concentrated followed by immunoblotting or Coomassie staining for BSA.

modifier A (CrmA) protein, an inhibitor of caspase-1 and caspase-8 (Rodriguez *et al*, 2003); whereas ecto-CRT induction by anthracyclines was suppressed (Figure 6B). Moreover, shRNA-based stable depletion of caspase-8 in CT26 cancer cells (Supplementary Figure S11A) abolished anthracycline-induced ecto-CRT without affecting Hyp-PDT-induced ecto-CRT (Figure 6C). Thus, while caspase-8 is involved in the canonical CRT pathway as reported previously (Panaretakis *et al*, 2009), it is dispensable for induction of ecto-CRT by phox-ER stress.

On the other hand, while cells lacking BAX/BAK showed a compromised ability to surface expose CRT in response to both anthracyclines and Hyp-PDT (Figure 6D); yet, they did not show any defect in secretion of ATP following Hyp-PDT (Figure 6E). The intracellular levels of ATP were not affected by the absence of BAX/BAK (data not shown). For cells

 

lacking BAX/BAK, it has been suggested that their reduced steady-state levels of ER-$Ca^{2+}$ (Scorrano *et al*, 2003) might play an important role in ecto-CRT induction (Tufi *et al*, 2008; Panaretakis *et al*, 2009). Hyp-PDT has been observed to induce rapid ER-$Ca^{2+}$ depletion, which causes a rise in $[Ca^{2+}]_{Cyt}$ (Buytaert *et al*, 2006); however, chelation of cytosolic $Ca^{2+}$ with BAPTA-AM did not affect the surface mobilization of CRT induced by Hyp-PDT (Supplementary Figure S11B). Moreover, overexpressing SERCA2 in cells lacking BAX/BAK (DKO/SERCA↑ cells) could not restore their ability to induce ecto-CRT (Supplementary Figure S11C). Here, SERCA2 overexpression is supposed to correct the low resting $[Ca^{2+}]_{ER}$ in cells lacking BAX/BAK (Scorrano *et al*, 2003). Thus, we can assume that $[Ca^{2+}]_{Cyt}$ does not govern ecto-CRT induction after exposure to phox-ER stress, and that SERCA2 overexpression in cells lacking BAX/BAK does not restore ecto-CRT.

Based on these observations, we conclude that induction of ecto-CRT by phox-ER stress follows a molecular pathway orchestrated chiefly by PERK and BAX/BAK, and that this pathway does not require caspases, eIF2α phosphorylation or increased $[Ca^{2+}]_{Cyt}$. On the other hand, following phox-ER stress, ATP is secreted independently of BAX/BAK in a PERK-dependent manner.

### *Ecto-CRT docks on the surface of ER-stressed cells predominantly via LRP1*

The identity of the biological entity/surface receptor that docks ecto-CRT is unknown (Zitvogel *et al*, 2010b). Ecto-CRT colocalizes at least partly with plasma membrane regions rich in GM-1 gangliosides (Gardai *et al*, 2005); hence, we hypothesized that ecto-CRT might bind to the lipid rafts. Since cholesterol is crucial for the stability of lipid rafts we used a cholesterol-depleting agent, methyl-β-cyclodextrin (MBC), to study the surface translocation of CRT in treated cells (Nyasae *et al*, 2003; Lancaster and Febbraio, 2005). MBC-based destabilization of lipid rafts resulted in decreased MTX-induced ecto-CRT. In contrast, Hyp-PDT-induced ecto-CRT was increased to a certain extent (Figure 7A). These results indicate that correct organization of lipid rafts is not necessary for phox-ER stress-induced ecto-CRT.

To identify the surface receptor for ecto-CRT, we performed an *in-silico* search for candidate molecules. We assumed that a candidate receptor would have two properties: (i) it is a common surface protein in at least human and mouse and (ii) it has a higher affinity for ecto-CRT than for other major KDEL-containing ER proteins. The *in-silico* approach consisted of functional predictions (protein–protein binding) derived from protein network analysis carried out by using the STRING (Search Tool for the Retrieval of Interacting Genes/Proteins) database and web-tool available at http://string-db.org/ (Jensen *et al*, 2009). Analysis of the overall binding interaction networks for both human (Supplementary Figure S12A) and murine CRT (Supplementary Figure S12B) identified low-density lipoprotein receptor-related protein 1 (LRP1 or CD91) as a potential candidate receptor. Consequently, to look for a competitive protein–protein interaction network for LRP1 and KDEL-containing proteins, we assembled the human (Supplementary Figure S12C) and the murine LRP1 (Supplementary Figure S12D) into separate networks with the respective major KDEL-containing ER proteins, including PDI, ERp72, CRT, ERp57, Bip/GRP78, HSP47, GRP94, P4HB, RCN1, and RCN2. This analysis revealed that CRT is one of the KDEL-containing proteins with which LRP1 consistently interacts in both human and mouse, *in silico*.

To translate these *in-silico* results into *in-vitro* setting, we used cells that are LRP1 competent ($LRP1^{+/+}$ MEF) or either partially ($LRP1^{+/-}$ MEF) or completely LRP1 deficient ($LRP1^{-/-}$ MEF) (Willnow and Herz, 1994; Roebroek *et al*, 2006). We treated these cells with Hyp-PDT or MTX and analysed the levels of ecto-CRT as well as 'secreted' or exo-CRT. These studies revealed that cells lacking LRP1 display low levels of ecto-CRT following MTX or Hyp-PDT treatment (Figure 7B). Correspondingly, the amounts of secreted CRT (or exo-CRT) increased in these treated cells lacking LRP1 (Figure 7C) in the absence of plasma membrane permeabilization (data not shown). Interestingly, we observed that while untreated and MTX-treated cells maintained a steady-state level of secreted CRT in WT conditions, yet Hyp-PDT-treated cells reduced the detectable levels of secreted CRT (Figure 7C). It is worth mentioning here that the presence of secreted CRT in untreated conditions is well documented (Patel *et al*, 1999). Moreover, the presence or absence of secreted CRT tends to vary from one ER stressor to another (Peters and Raghavan, 2011). Specifically in case of Hyp-PDT, not just the overall secreted CRT content but also the total extracellular secretory protein content was reduced considerably (data not shown), thereby pointing towards a (as yet unexplained) general decrease in 'secreted proteins' after low-dose Hyp-PDT.

Kinetically, a decrease in LRP1 levels reduced overall ecto-CRT, while increasing its active secretion (exo-CRT) after MTX (Figure 7E) or Hyp-PDT treatment (Figure 7F). Likewise, shRNA-based knockdown of LRP1 in CT26 cancer cells (Supplementary Figure S13A) suppressed the surface exposure of CRT (Figure 7G). Moreover, decrease in ecto-CRT was also observed in LRP1-deficient CHO cells (Supplementary Figure S13B and C), while LRP1 reconstitution (Supplementary Figure S13B) restored ecto-CRT (Supplementary Figure S13C). Coincidently, this reconstitution was accompanied by slight LRP1 overexpression (Supplementary Figure S13B), which interestingly correlated with overall increase in ecto-CRT as compared with the WT LRP1 CHO cells (Supplementary Figure S13C). Thus, we can conclude that LRP1-rich areas are predominant surface docking sites for ecto-CRT, at least after phox-ER stress.

### *Depletion of PERK, PI3K p110α, and LRP1 but not caspase-8 reduces immunogenicity of phox-ER stressed dead/dying cancer cells*

The *in-vitro* data discussed above indicate that for phox-ER stress-induced ecto-CRT, caspase-8 is dispensable but PERK, PI3K p110α, and LRP1 are crucial at various levels (Figure 8A). In fact, PERK and PI3K p110α were also found to be required for active ATP secretion (Figure 8A). In light of these *in-vitro* observations, we hypothesized that PERK, PI3K p110α, and LRP1 but not caspase-8 might be crucial for the immunogenicity of phox-ER stressed cancer cells. To verify this hypothesis *in vivo*, we decided to take advantage of the CT26 mice immunization model (Figure 1E; Supplementary Figure S5). Mice immunized with Hyp-PDT-treated CO-shRNA CT26 cells were highly efficient in resisting tumour growth at the rechallenge sites injected with live, untreated CT26 cells as opposed to non-immunized CNTR mice

(Figure 8B). This is a sign of high immunogenicity leading to the activation of the adaptive immune system as observed for the WT CT26 cells (Figure 1G). In line with the *in-vitro* observations, when immunization was carried out with Hyp-PDT-treated CT26 cells stably expressing the caspase-8 shRNA, the immunogenicity of these treated cells was not compromised (Figure 8B). In contrast, mice immunized with Hyp-PDT-treated CT26 cells stably expressing shRNA against either PERK, PI3K p110α, or LRP1 showed attenuated resistance to tumour growth at the rechallenge site, thereby pointing towards reduced immunogenicity of these dead/dying CT26 cells (Figure 8B). Depletion of PERK and PI3K

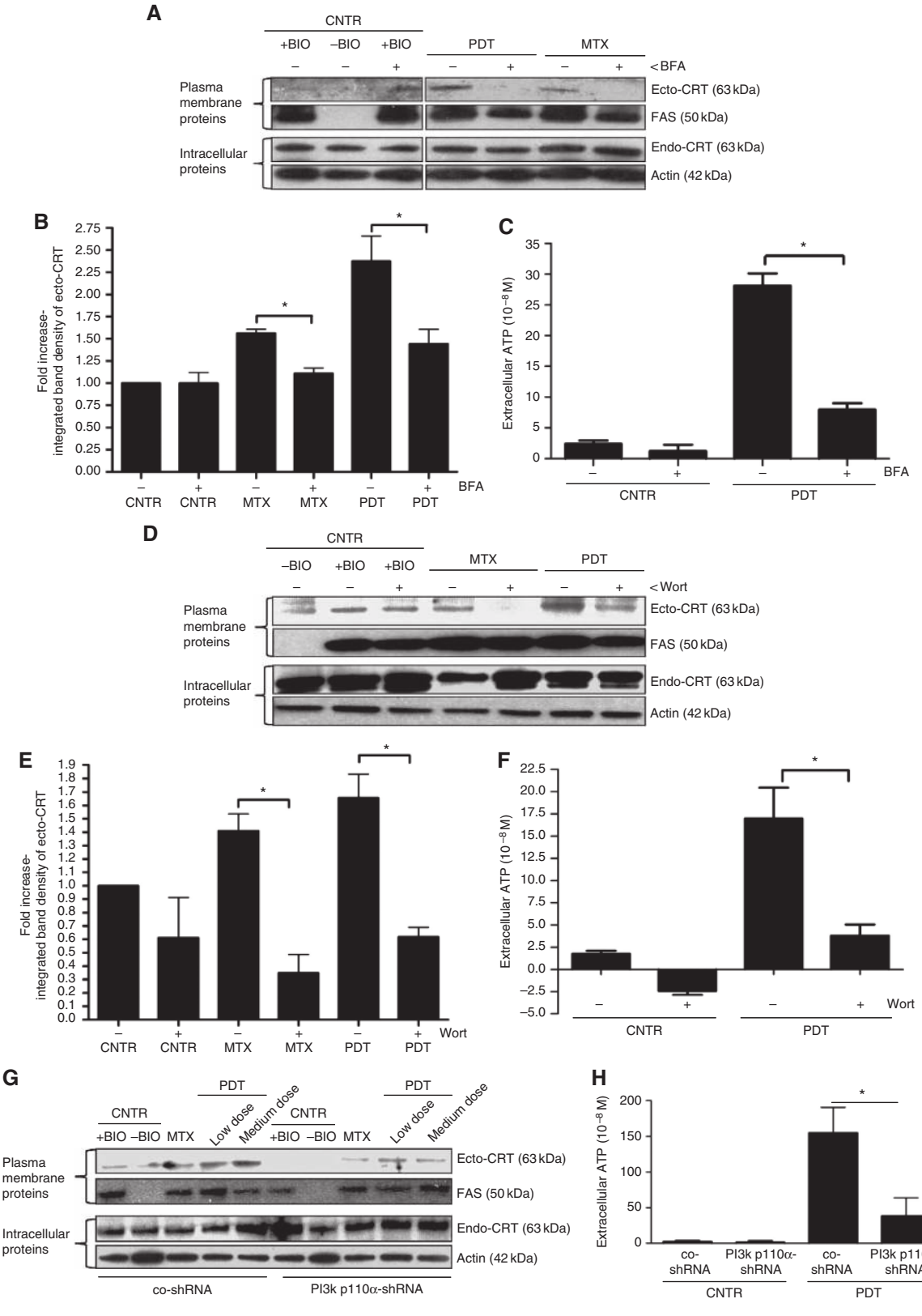

p110α impaired immunogenicity of phox-ER stressed dying/dead CT26 cells to a relatively larger extent than LRP1 depletion. Overall, based on these results we can conclude that PERK, PI3K p110α and to some extent LRP1 are crucial while caspase-8 is dispensable for mediating phox-ER stress-induced immunogenicity of dying/dead cancer cells.

## Discussion

In the current study, we observed that cell death induced by phox-ER stress endows tumour cells with the major properties of immunogenic apoptosis, including: induction of ecto-CRT, active secretion of ATP, phenotypic maturation ($CD80^{high}$, $CD83^{high}$, $CD86^{high}$, $MHC\text{-}II^{high}$), and functional stimulation ($NO^{high}$, $IL\text{-}10^{absent}$, $IL\text{-}1\beta^{high}$) of DCs as well as activation of the adaptive immune system, *in vivo*.

Surface-exposed CRT was induced by phox-ER stress before biochemical signs of apoptosis became apparent and in that it resembled ecto-CRT induction described for anthracyclines (Panaretakis *et al*, 2009). The anthracycline-induced ecto-CRT translocation pathway has been shown to depend on PERK-mediated eIF2α phosphorylation (eIF2α-P), followed by caspase-8-mediated BAP31-dependent activation of BAX/BAK proteins (Panaretakis *et al*, 2009). However, we observed that the pathway governing ecto-CRT induction by phox-ER stress differed markedly from the 'canonical CRT pathway', as only PERK and BAX/BAK were required for it (Supplementary Figure S14). The apparent dispensability of eIF2α-P and caspase-8, or of caspase signalling in general, indicates that ecto-CRT induction by phox-ER stress is orchestrated by a different pathway. In fact, these observations downplay the role of UPR signalling as well as ER-proximal partial caspase activation during phox-ER stress. We further explored the mechanism of ecto-CRT exposure and found that for anthracyclines and phox-ER stress, the classical secretory pathway and PI3 kinase-dependent plasma membrane trafficking was involved in ecto-CRT translocation (Supplementary Figure S14). Interestingly, SNARE-based exocytosis has also been implicated in the canonical CRT pathway thereby substantiating the role of plasma membrane trafficking in this process (Panaretakis *et al*, 2009). Additionally, we found that the KDEL sequence of ecto-CRT is not proteolytically removed (Krysko and Vandenabeele, 2008) but is carried with it onto the surface, and that ERp57 is not found 'complexed' with ecto-CRT as has been reported for the anthracycline-mediated translocation pathway (Obeid *et al*, 2007; Panaretakis *et al*, 2009). Intriguingly, this study also sheds new light on the elusive mechanism of surface tethering of CRT (Supplementary Figure S14). We show that LRP1-deficient/depleted cells have impaired ability to properly dock CRT on their surface and that this defect is independent from the stress-specific translocation pathway.

Furthermore, we characterized the molecular mechanisms underlying the secretion of another crucial DAMP, secreted ATP, for which no clear-cut pre-apoptotic mechanism has been proposed yet (Aymeric *et al*, 2010). Previously, secreted ATP has been mostly associated with mechanical/osmotic strain (Nandigama *et al*, 2006), cells in early apoptotic stages, during which caspases are active (Elliott *et al*, 2009; Chekeni *et al*, 2010) or in mid apoptotic stages, coincident with nuclear fragmentation (Ghiringhelli *et al*, 2009; Martins *et al*, 2009).

We report for the first time that ATP is secreted by stressed cells at a stage that can be considered clearly pre-apoptotic. We also observed that the concentration of this secreted ATP after phox-ER stress differed from one cell type to another. Importantly, we also show that induction of ATP secretion by phox-ER stress is dependent on PERK but independent of BAX/BAK (Supplementary Figure S14). Furthermore, this process of ATP secretion also involves the secretory pathway and PI3 kinase-dependent extracellular trafficking (Supplementary Figure S14), which makes this pathway different from the ATP secretion pathway instigated during the early apoptotic stage (Chekeni *et al*, 2010). This also points to ER/Golgi as the possible sources of secreted ATP. Interestingly, we observed that following phox-ER stress, intracellular ATP levels are increased in the pre-apoptotic stage, as reported for certain other apoptotic stimuli (Zamaraeva *et al*, 2005). We suspect that this could be due to the increased ER-mitochondrial coupling following ER stress favouring the enhanced uptake of $Ca^{2+}$ by the mitochondria (Bravo *et al*, 2011), a phenomenon that we also observe following phox-ER stress (Verfaillie *et al*, unpublished data). Thus, after phox-ER stress, both DAMPs (ecto-CRT and secreted ATP) follow overlapping pathways to reach the extracellular space (Supplementary Figure S14). These overlapping paths are probably part of a specific danger-signalling system that acts well before signs of apoptosis become manifested. Moreover, it should also be noted that

**Figure 4** Induction of ecto-CRT and ATP secretion by phox-ER stress occurs *via* secretory pathway and PI3 kinase-dependent plasma membrane/extracellular trafficking. (**A**, **B**) Induction of ecto-CRT by phox-ER stress is sensitive to Brefeldin A (BFA). T24 cells were preincubated with 10 μM of BFA for 1 h followed by treatment with a medium PDT dose, MTX (1 μM for 4 h) or left untreated (CNTR) and recovered 1 h post PDT. Surface proteins were biotinylated and immunoblotted (**A**). In (**A**), (**D**), and (**G**), '+BIO' indicates controls exposed to buffer with biotin and '−BIO' indicates controls exposed to buffer without biotin (negative control). Also, the integrated density of the ecto-CRT protein band was quantified by Image J software (**B**). In (**B**) and (**E**), data have been normalized to CNTR values; fold change values are mean values of three independent experiments ± s.e.m. ($^*P<0.05$). (**C**) ATP secretion following phox-ER stress is sensitive to BFA. T24 cells were preincubated with 10 μM of BFA for 1 h and then treated with medium PDT dose. The resulting conditioned media (1 h post PDT in serum-free media) were analysed for the presence of ATP. Absolute concentrations are means of two independent experiments (five replicate determinations in each) ± s.d. ($^*P<0.05$). (**D**, **E**) Induction of ecto-CRT by phox-ER stress is sensitive to Wortmannin (Wort). T24 cells were preincubated with 100 nM of Wort for 1 h and then treated with a medium PDT dose or MTX (1 μM for 4 h). Cells were recovered 1 h post PDT. This was followed by biotinylation of the surface proteins (**D**) and measurement of the integrated density of ecto-CRT protein bands (**E**) as detailed in (**A**) and (**B**), respectively. (**F**) ATP secretion following phox-ER stress is sensitive to Wort. T24 cells were preincubated with 100 nM Wort for 1 h and then treated with medium PDT dose. The resulting conditioned media (1 h post PDT in serum-free media) were analysed for the presence of ATP as detailed in (**C**). (**G**) PI3K p110α shRNA decreases phox-ER stress-induced ecto-CRT. CO-shRNA CT26 cells and CT26 expressing PI3K p110α shRNA 3 were treated with indicated PDT doses or MTX (1 μM for 4 h). They were recovered 1 h post PDT followed by biotinylation of the surface proteins as detailed in (**A**). (**H**) ATP secretion following phox-ER stress is reduced by PI3K p110α shRNA. CO-shRNA CT26 cells and CT26 expressing PI3K p110α shRNA 3 were treated with medium PDT dose. The resulting conditioned media (1 h post PDT in serum-free media) were analysed for the presence of ATP. Absolute concentrations are means of five replicate determinations ± s.d. ($^*P<0.05$).

while ecto-CRT induction (Obeid *et al*, 2007; Panaretakis *et al*, 2009) and optimal ATP secretion (Martins *et al*, 2009) require different doses of anthracyclines, in the case of Hyp-PDT they are dose associated (i.e., induced by similar doses), thereby integrating the emergence of these two critical immunogenic signals within a single therapeutic set-up.

Interestingly, we observed that absence or depletion of PERK compromised the ability of phox-ER stressed cells to modulate their extracellular secretory protein content. This along with the emerging evidence of PERK's role in proper secretory pathway functioning (Gupta *et al*, 2010; Teske *et al*, 2011) might imply that PERK could be regulating ecto-CRT

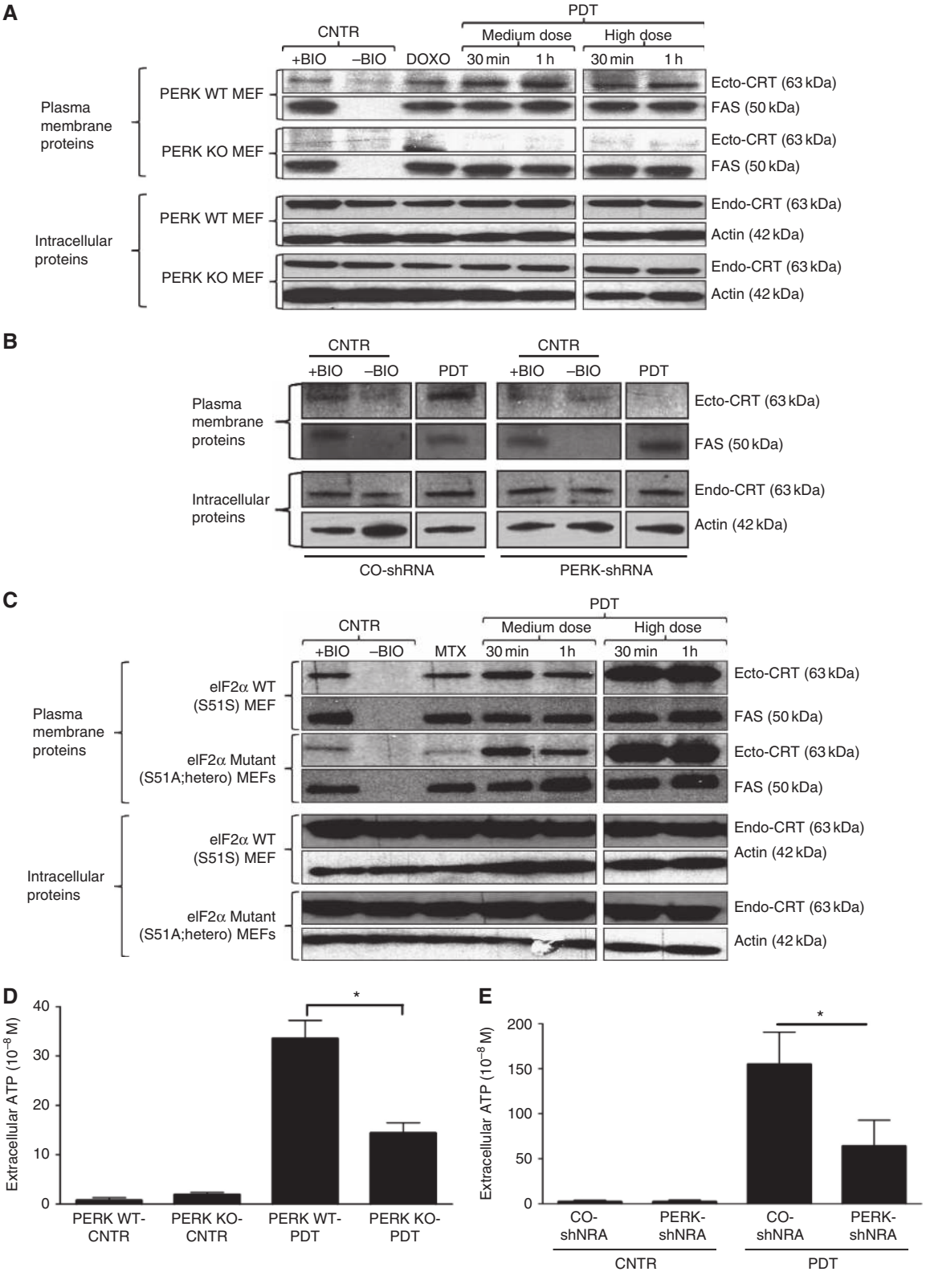

induction and ATP secretion by governing the proper functioning of the secretory pathway after phox-ER stress; a premise that warrants systematic investigation in the near future. On the other hand, the role of BAX/BAK proteins in ecto-CRT induction is less clear. A recent study has shown that these pro-apoptotic proteins regulate ER membrane permeability in ER-stressed cells (Wang *et al*, 2011b). Modulation of ER membrane permeability could expedite or assist in the delivery of ER luminal proteins, such as CRT, to the cell surface. However, more research is required to ascertain the link between BAX/BAK and phox-ER stress-induced ecto-CRT.

The depletion of PERK, PI3K p110α, and LRP1 (to a relatively lesser extent) reduced the immunogenicity of phox-ER-stressed cancer cells *in vivo*. The milder effect of LRP1 depletion on immunogenicity could probably be explained by the fact that even extracellularly secreted, non-surface tethered form of CRT can mediate DC maturation (Bajor *et al*, 2011) and antitumour immunity (Wang *et al*, 2011a). However, in contrast to previous observations for anthracyclines (Panaretakis *et al*, 2009), depletion of caspase-8 had no effect on phox-ER stress-induced immunogenicity. These *in-vivo* observations further reinforce the novel molecular pathway observed for phox-ER stress-induced ecto-CRT, *in vitro*. Importantly, depletion of PERK, PI3K p110α, and LRP1 did not completely abolish the immunogenicity of cancer cells responding to phox-ER stress meaning thereby that (1) either a minor residual exposure/secretion of DAMPs regulated by these signalling molecules is sufficient for conferring a particular degree of immunogenicity or (2) there are additional yet-to-be-described danger signals non-dependent on these pathway components that contribute to phox-ER stress-induced immunogenicity.

In conclusion, this study shows that phox-ER stress leads to the generation of the immunological and molecular hallmarks of immunogenic apoptosis in cancer cells. Our findings expand the set of experimental anticancer treatments that can induce immunogenic cell death by adding Hyp-PDT. We also demonstrate for the first time that two DAMPs, ecto-CRT and secreted ATP, can be 'emitted' in the 'pre-apoptotic' phase of cell death through a common molecular pathway in which PERK, an ER stress sensor, is at the signalling core. This is the first report on two critical DAMPs following overlapping molecular pathways to reach the extracellular space. Moreover, our study suggests that the LRP1-rich areas might be the elusive surface docking entities for ecto-CRT on the dying cancer cell surface.

In a more general sense, an important conclusion that can be derived from our study is that the emission of key DAMPs, like ecto-CRT and secreted ATP, by cancer cells can occur through mechanisms that are evidently stress specific. The dispensability of caspase signalling for the mobilization of DAMPs and immunogenic apoptosis induced by phox-ER stress is also a novel observation. It implies that emission of danger signals by the stressed cancer cells is a phenomenon mediated by a separate ROS and ER stress-mediated subroutine, which occurs in parallel to apoptosis induction. This is a premise that deserves to be substantiated in further investigations and which may have important implications for the development of new treatment modalities harnessing the immunogenicity of the cancer cells.

## Materials and methods

### *Materials and reagents*

Hypericin was prepared, purified, and stored as described previously (Buytaert *et al*, 2006). Z-Val-Ala-Asp(OMe)-fmk (zVAD-fmk) was purchased from Bachem (Weil am Rhein, Germany). Latrunculin B (LanB) and 1,2-bis(2-aminophenoxy)ethane-N,N,N′,N′-tetracetate acetyloxy methylester (BAPTA-AM) were purchased from Invitrogen (Carlsbad, CA, USA). Brefeldin A (BFA), L-Histidine (L-Hist), Mitoxantrone (MTX), Doxorubicin (DOXO), Nocodazole (Noco), and Wortmannin (Wort) were purchased from Sigma (St Louis, MO, USA). Methyl-β-cyclodextrin (MBC) was a kind gift from Prof. J Swinnen (Catholic University of Leuven, Belgium). Antibodies against ERp57, CHOP, P-eIF2α, eIF2α, HSP90, caspase 3, Bip/GRP78, and PERK were purchased from Cell Signaling Technology (Danvers, MA, USA). Anti-calnexin antibody was purchased from Stressgen (Victoria, BC, Canada). Anti-calreticulin antibodies were purchased from Stressgen or Pierce. Rabbit polyclonal antibody (1704) recognizing the C-terminus of the LRP1 protein has been described previously (Reekmans *et al*, 2010). Anti-PI3K p110α antibody was purchased from Pierce. Anti-caspase-8 antibody was purchased from Alexis Biochemicals (San Diego, CA, USA). Anti-$Na^+/K^+$ ATPase antibody was purchased from Novus Biologicals (Littleton, CO, USA). Anti-FAS/CD95 (N-18, M-20, and C-20), anti-ICAM-1, and anti-HSP70 antibodies were purchased from Santa Cruz Biotech (Santa Cruz, CA, USA). Anti-actin antibody was purchased from Sigma. Antibody against the KDEL sequence was purchased from Abcam (Cambridge, UK). Anti-PARP antibody was purchased from BD Pharmingen (San Jose, CA, USA). Anti-CD47 antibody was purchased from ImmunoTools (Friesoythe, Germany). Secondary antibodies conjugated to horseradish peroxidase were purchased from Cell Signaling Technology or Abcam.

### *Cell lines and induction of photo-oxidative (phox)-ER stress and/or immunogenic apoptosis*

T24, CT26, HeLa, and MEF cells were cultured at 37°C under 5% $CO_2$ in DMEM containing 4.5 g/l glucose and 0.11 g/l sodium pyruvate and supplemented with 2 mM glutamine, 100 units/ml penicillin, 100 μg/l streptomycin and 10% fetal bovine serum (referred to as normal culture medium hereafter). CHO cells were

**Figure 5** Induction of ecto-CRT and ATP secretion by phox-ER stress are PERK dependent. (**A**) Induction of ecto-CRT by phox-ER is reduced in the absence of PERK. MEF cells containing PERK (WT) or lacking it (KO) were treated with PDT, DOXO (25 μM for 4 h) or left untreated (CNTR). They were recovered at the indicated time points post-PDT. Surface proteins were biotinylated and immunoblotted. In (**A–C**), '+BIO' indicates controls exposed to buffer with biotin and '−BIO' indicates controls exposed to buffer without biotin (negative control). (**B**) Induction of ecto-CRT by phox-ER is reduced by PERK shRNA. CO-shRNA CT26 cells and CT26 expressing PERK shRNA 3 were treated with medium PDT dose and recovered 1 h post PDT followed by surface biotinylation as detailed in (**A**). (**C**) Ecto-CRT induced by phox-ER stress is not affected by the presence of non-phosphorylable eIF2α. MEF cells expressing normal eIF2α (WT) or a non-phosphorylable mutant heterozygously (S51A knock-in mutation) were treated with PDT or MTX (1 μM for 4 h) and recovered at the indicated time points. This was followed by surface biotinylation as detailed in (**A**). (**D**) PERK deficiency decreases phox-ER stress-induced secreted ATP. MEF cells that were PERK WT or PERK KO were treated with a medium PDT dose. The resulting conditioned media (1 h post PDT in serum-free media) were analysed for the presence of ATP. Absolute concentrations are mean values of two independent experiments (five replicate determinations in each) ± s.d. ($^*P<0.05$). (**E**) PERK depletion decreases phox-ER stress-induced secreted ATP. CO-shRNA CT26 cells and CT26 expressing PERK shRNA 3 were treated with a medium PDT dose. The resulting conditioned media (1 h post PDT in serum-free media) were analysed for the presence of ATP. Absolute concentrations are mean values of five replicate determinations ± s.d. ($^*P<0.05$).

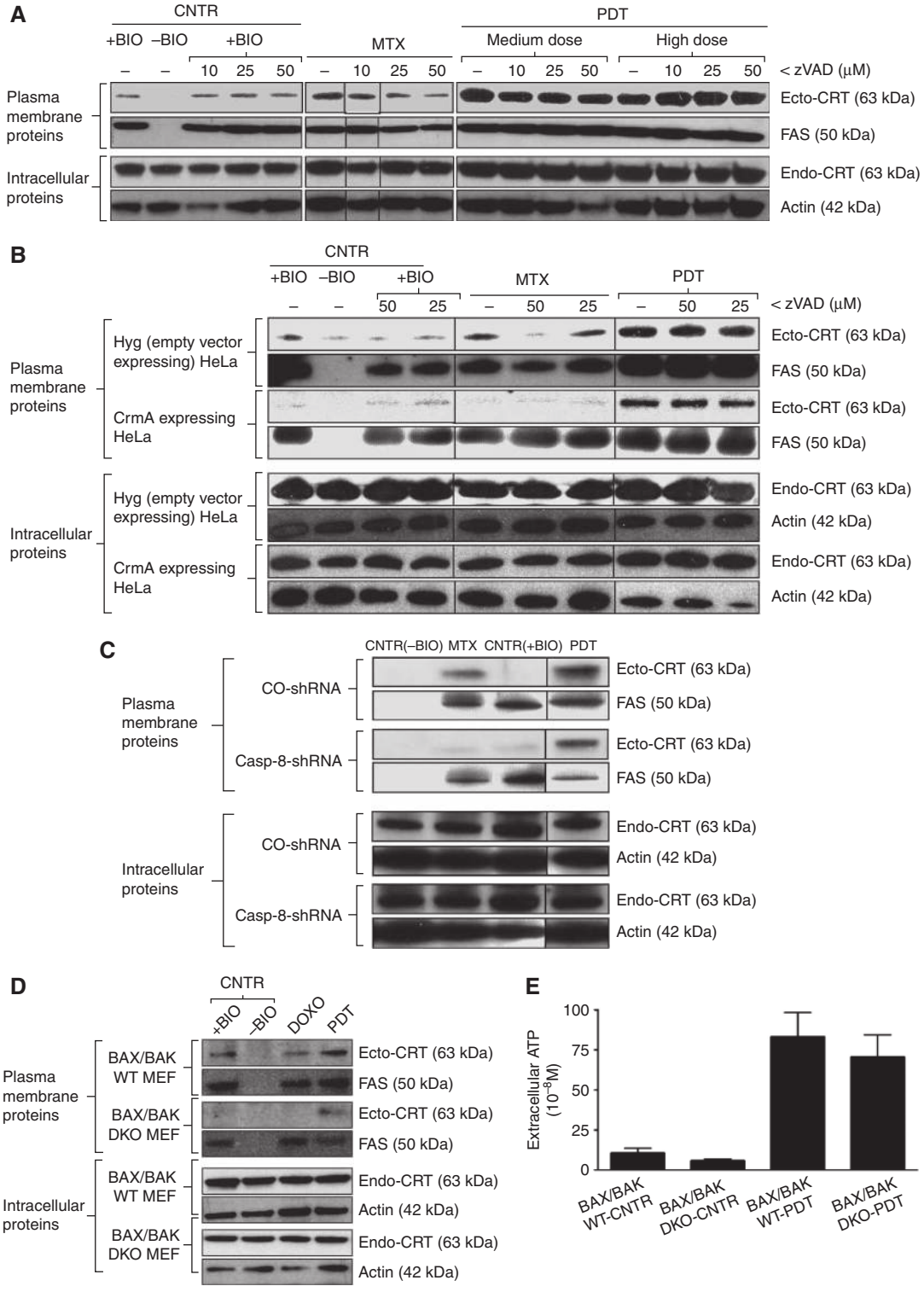


**Figure 6** Ecto-CRT induced by phox-ER stress is caspase-8 independent but BAX/BAK dependent. (**A**) Ecto-CRT induced by phox-ER stress is caspase independent. T24 cells were preincubated with 0, 10, 25, or 50 μM of zVAD for 1 h and then treated with PDT, MTX (1 μM for 4 h) or left untreated (CNTR), and recovered 1 h post PDT. Surface proteins were biotinylated and immunoblotted. In (**A**–**D**), '+BIO' indicates controls exposed to buffer with biotin and '−BIO' indicates controls exposed to buffer without biotin (negative control). (**B**) Ecto-CRT induced by phox-ER stress is caspase-8 independent. HeLa cells expressing empty vector Hyg or CrmA were preincubated with 0, 25, or 50 μM of zVAD for 1 h, then treated with a high PDT dose or MTX (1 μM for 4 h) and recovered 1 h post PDT. This was followed by biotinylation as explained in (**A**). (**C**) Induction of ecto-CRT by phox-ER is not affected by casp-8 shRNA. CO-shRNA CT26 cells and CT26 expressing casp-8 shRNA 1 were treated with medium PDT dose or MTX (1 μM for 4 h) and recovered 1 h post PDT followed by surface biotinylation as detailed in (**A**). (**D**) Ecto-CRT induced by phox-ER stress is BAX/BAK dependent. MEF cells either containing BAX/BAK (WT) or lacking it (DKO) were treated with a medium PDT dose or DOXO (25 μM for 4 h) and recovered 30 min post PDT. This was followed by surface biotinylation as detailed in (**A**). (**E**) BAX/BAK deficiency does not affect phox-ER stress-induced secreted ATP. MEF cells that were BAX/BAK WT or DKO were treated with a medium PDT dose. The resulting conditioned media (1 h post PDT in serum-free media) were analysed for the presence of ATP. Absolute concentrations are mean values of two independent experiments (five replicate determinations in each) ± s.d.

 

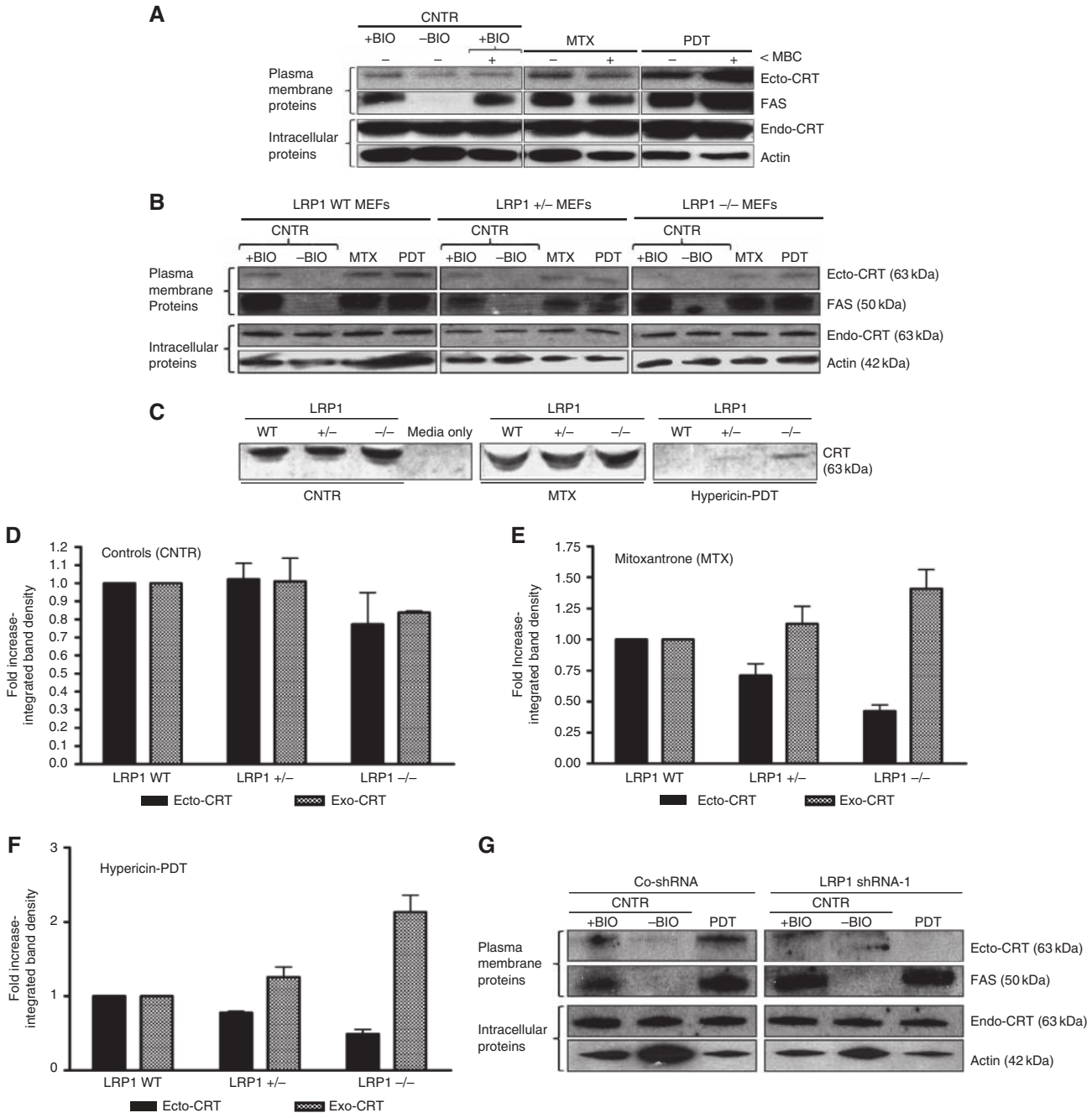


**Figure 7** Ecto-CRT induced by phox-ER stress docks on the surface *via* the LRP1 molecule. (**A**) Ecto-CRT induced by phox-ER stress is not dependent on lipid rafts. T24 cells were preincubated with 2 μM of MBC for 1 h and then treated with a medium PDT dose, MTX (1 μM for 1 h) or left untreated (CNTR). They were recovered 5 min post PDT. Surface proteins were biotinylated and immunoblotted. In (**A**), (**B**), and (**G**), '+BIO' indicates controls exposed to buffer with biotin and '−BIO' indicates controls exposed to buffer without biotin (negative control). (**B**–**F**) Ecto-CRT retention on ER-stressed cancer cells is dependent on the level of LRP1. MEF cells containing levels of 100% LRP1 (LRP1 WT), 50% LRP1 (LRP1 +/−), or 0% LRP1 (LRP−/−) were treated with a low PDT dose or MTX (1 μM for 4 h in serum-free media) followed by recovery in serum-free media after 1 h post PDT. Surface proteins were biotinylated and immunoblotted (**B**) as detailed in (**A**). Simultaneously, the conditioned media (CM) derived from these cells were concentrated and immunoblotted (**C**). The integrated density of CRT protein bands in (**B**) and (**C**) was quantified by Image J software for untreated (**D**), MTX-treated (**E**), and PDT-treated (**F**) conditions: where black is for ecto-CRT bands in the immunoblots of biotinylated surface proteins and grey is for 'exo-CRT' bands in the immunoblots of concentrated CM. Data have been normalized to the respective LRP1 WT values. Fold change values are means of three independent experiments ± s.e.m. (**G**) Induction of ecto-CRT by phox-ER stress is reduced by LRP1 shRNA. CO-shRNA CT26 cells and CT26 expressing LRP1 shRNA 1 were treated with medium PDT dose and recovered 1 h post PDT followed by surface biotinylation as detailed in (**A**).

cultured in HAM-F12 media supplemented with 2 mM glutamine, 100 units/ml penicillin, 100 μg/l streptomycin, and 10% fetal bovine serum. BAX/BAK DKO (double knock-out) MEF cells overexpressing SERCA2 were maintained in culture medium containing 2 μg/ml puromycin (Invivogen, San Diego, CA, USA). Mf4/4 mouse macrophages were cultured in RPMI-1640 medium supplemented with 10% fetal calf serum, 100 units/ml penicillin, 2 mM glutamine, 1 mM sodium pyruvate and $2 \times 10^{-5}$ mM β-mercaptoethanol. JAWSII mouse DC line was cultured in RPMI-1640 medium supplemented with 10% fetal calf serum, 100 units/ml penicillin, 2 mM glutamine and 5 ng/ml granulocyte macrophage-colony stimulating factor (GM-CSF; PeproTech, Rocky Hill, NJ, USA).

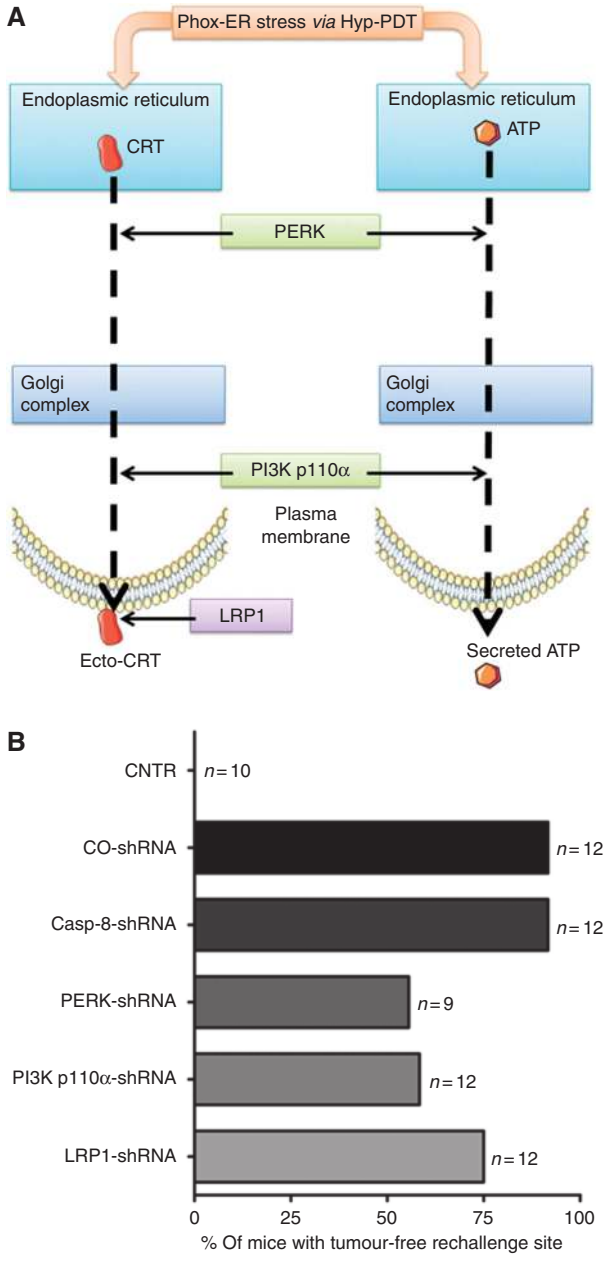


**Figure 8** Depletion of PERK, PI3K p110α, and LRP1 but not caspase-8 reduces phox-ER stress-induced immunogenicity. (**A**) Hypothetical representation of main molecular players in phox-ER stress-induced ecto-CRT and ATP secretion pathways. *In-vitro* data suggested that while caspase-8 was dispensable for ecto-CRT induction after phox-ER stress; PERK and PI3K p110α were indispensable. In fact, both of these latter molecules were also required for ATP secretion. Moreover, LRP1 was observed to be crucial for surface tethering of ecto-CRT. (**B**) The mice were immunized either with PBS (CNTR) or with highest PDT dose treated CO-shRNA CT26 cells or with different CT26 cells expressing casp-8 shRNA 1, PERK shRNA 3, PI3K p110α shRNA 3, or LRP1 shRNA 1, also treated with the highest PDT dose. These 'immunized' mice were then rechallenged with live CT26 tumour cells. Subsequently, the percentage of mice with tumour-free rechallenge site was determined ($n$ represents the number of mice).

For induction of immunogenic apoptosis, the cells were cultured in the presence of MTX (1 μM) or DOXO (25 μM). Phox-ER stress was induced by Hypericin-based PDT (Hyp-PDT). For Hyp-PDT (unless otherwise mentioned), T24 and CT26 cells were incubated with 150 nM Hypericin (for 16 h in normal culture medium), HeLa cells were incubated with 125 nM Hypericin (for 16 h in normal culture medium), CHO cells were incubated with 200 nM Hypericin (for 16 h in normal culture medium), while MEF cells were incubated with 200 nM Hypericin (for 2 h in serum-free culture medium). Irradiation was performed as described previously (Vantieghem *et al*, 1998). Four Hyp-PDT doses, based on the light fluence, were defined as low PDT dose (fluence = 0.54 J/cm$^2$), medium PDT dose (1.35 J/cm$^2$), high PDT dose (2.16 J/cm$^2$), and the highest PDT dose (2.70 J/cm$^2$). For, Photofrin-based PDT (PF-PDT), the T24 cells were incubated with 10 μg/ml Photofrin (for 24 h in normal culture medium) and irradiated at a fluence of 0.48 J/cm$^2$. Cells loaded with Hypericin or Photofrin were handled in either dark or subdued light (<1 μW/cm$^2$). All the untreated or control (CNTR) sample conditions had Hypericin in absence of irradiation (i.e., absence of PDT treatment).

### *Generation of shRNA stable clones of CT26 cells*

All the TRC1 shRNA clones were in lentiviral pLKO.1-puro vector (Sigma-Aldrich, St. Louis, MO, USA) and were obtained from the BCCM/LMBP Plasmid collection, Department of Biomedical Molecular Biology, Ghent University, Belgium (http://bccm.belspo.be/about/lmbp.php). An empty pLKO.1-puro control vector was used as a control (CO-shRNA) (BCCM/LMBP Plasmid collection). Three shRNAs targeted against each of the four murine mRNA types coding for proteins like LRP1, PI3K p110α, PERK, and caspase-8, respectively, were used. Sequences of these shRNAs are mentioned in Supplementary Table S1. To generate lentivirus particles, HEK 293T cells were seeded in 25 cm$^2$ flasks at $1.3 \times 10^6$ cells per 4 ml and transfected the following day by the calcium phosphate method with 4 μg of pLKO.1-puro carrying the respective shRNAs or with empty pLKO.1-puro. Each transfection also included 1.2 μg of a plasmid encoding VSV-G (pMD2-VSV-G, Tronolab) and 2.6 μg of a plasmid encoding packaging proteins (pCMVdR8.9, Tronolab). After 6 h, the cells are washed with prewarmed PBS and 4 ml of fresh media was added. Twenty-four hours after transfection, the cells were placed at 32°C for another 24 h. VSV-G pseudotyped virus was collected 48 h after transfection, passed through 0.45 μm filters and then added to the exponentially growing CT26 cell cultures in the presence of 8 μg/ml of polybrene. Seven hours later a second infection was done. The cells were expanded and selected by puromycin treatment (9 μg/ml) for 3 days. Knockdown of LRP1, PI3K p110α, PERK, and caspase-8 was confirmed by immunoblotting.

### *In-vivo analysis of immune system priming in mice*

All mice were maintained in pathogen-free conditions and the experiments were performed according to the guidelines of the local Ethics Committee of Ghent University-VIB and KU Leuven. CT26 cells were incubated with MTX (1 μM), tunicamycin (TUN, 65 μM; Sigma-Aldrich) or exposed to the highest PDT dose of Hyp-PDT. After a 24-h recovery, $3 \times 10^6$ of these cells were injected subcutaneously (s.c.) in 200 μl of PBS into the left flank of 7-week-old female BALB/c mice from Janvier (Bio Services BV, The Netherlands). Immunization was done twice with a 10-day interval. Control mice were injected with 200 μl PBS. Mice were then rechallenged with $5 \times 10^5$ live untreated CT26 cells in the other (right) flank 7 days after the second immunization. The 'communication' of the tumour antigenic memory to the adaptive immune system was studied by analysing the incidence of tumours at the rechallenge site (i.e., in the right flank of the mice). Hence, following the rechallenge, the mice were monitored every 5–6 days for the presence of tumours at the rechallenge site and the experiment was stopped as soon as the tumours in control mice became unmanageable, that is, either necrotic or capable of causing movement problems (about 20–30 days). Absence of tumours at the rechallenge site was taken as a sign of 'priming' of the adaptive immune system for the antigens derived from the treated/dying/dead CT26 cells.

### *Analysis of human DC maturation, NO, and cytokines*

Human immature DCs (hu-iDCs) were isolated and cultured as described (Ferreira *et al*, 2009). T24 cells exposed to high Hyp-PDT treatment and AN (induced by one cycle of freeze thawing) were co-incubated with hu-iDCs at a ratio of 1:20 (hu-iDCs:T24) for 24 h. Hu-iDCs stimulated with 100 ng/ml of *Escherichia coli*-derived LPS for 24 h (Sigma) were used as positive controls for DC maturation. After detachment and washing, the cells were stained with the

following antibodies: FITC-conjugated anti-HLA-DR (MHC II) (Invitrogen, Merelbeke, Belgium) and APC-conjugated anti-CD86 (Invitrogen, Merelbeke, Belgium) or FITC-conjugated anti-CD80 (Beckton & Dickinson, Mountain View, CA, USA) and APC-conjugated anti-CD83 (Invitrogen, Merelbeke, Belgium) according to manufacturer's instructions. Anti-human IgG1 (Beckton & Dickinson) and anti-human IgG2b (Invitrogen, Merelbeke, Belgium) antibodies were used as isotype controls. After the antibody staining, the cells were washed and analysed with a FACSCalibur flow cytometer (Beckton & Dickinson). The conditioned co-culture media (CCM) derived from these hu-iDC and T24 cell co-incubation experiments were collected and stored for further analysis. NO in CCM was quantified by Griess assay (Becker *et al*, 2000). Immunoreactive levels of human IL-1β (MPXHCYTO-60K-04) and IL-10 (MPXHCYTO-60K-04) were measured in the CCM by using Milliplex human cytokines (Merck Millipore, Billerica, MA, USA). The samples were prepared according to manufacturers' instructions and analysed on Bio-Plex 200 Systems (Bio-Rad, Hercules, CA, USA).

#### *ATP assays*

The cells were treated as indicated. Extracellular ATP was measured in the conditioned (serum-free) media and intracellular ATP was determined after saponin-based lysis. We used an ATP Bioluminescent assay kit (Sigma) based on luciferin-luciferase conversion, following manufacturer's instructions. Bioluminescence was assessed by optical top reading *via* FlexStation 3 microplate reader (Molecular Devices Inc., Sunnyvale, CA, USA).

#### *Bioinformatics and statistical analysis*

Protein–protein binding interaction networks were generated using the STRING database (http://string-db.org/). Both predicted interactions and interactions supported by biochemical evidence or databases (including Reactome and Kyoto Encyclopedia of Genes and Genomes) were considered.

Data are presented in fold changes, absolute concentrations or percentages with mean ± s.d. or mean ± s.e.m. indicated in figure legends. All statistical analyses were performed using either Prism software (GraphPad Software, USA) or GraphPad QuickCalcs online software (http://www.graphpad.com/quickcalcs/index.cfm). Student's *t*-test was used for statistical analysis with significance level set at $P<0.05$.

#### *Supplementary data*

Supplementary data are available at *The EMBO Journal* Online (http://www.embojournal.org).

## Acknowledgements

We would like to thank Amin Bredan for excellent editorial assistance. We acknowledge the help of Dr Raf Ponsaerts (KU Leuven, Leuven, Belgium) with ATP measurements and Dr Johan Swinnen for kindly providing us with reagents. We thank Dr Peter Carmeliet (Vesalius Research Center, VIB, Leuven, Belgium) for the CT26 cells and Dr Marek Michalak (University of Alberta, Alberta, Canada) for the $CRT^{+/+}$ and $CRT^{-/-}$ MEF cells. This work was supported by a project from the Fund for Scientific Research Flanders (FWO-Vlaanderen, G.0728.10 to PA and DVK). Research in Agostinis' group is supported by grants from the KU Leuven (GOA/11/009). and FWO-Vlaanderen (G.0661.09). This paper presents research results of the IAP6/18, funded by the Interuniversity Attraction Poles Programme, initiated by the Belgian State, Science Policy Office. NR is a postdoctoral fellow supported by F.R.S-FNRS (grant F/5/4/5-MCF/KP). DVK is a postdoctoral fellow and AK is a doctoral fellow, both paid by fellowships from FWO-Vlaanderen. Research in Vandenabeele's group is supported by VIB, Ghent University (GROUP-ID consortium of the UGent MRP initiative), FWO-Vlaanderen (G.0875.11 and G.0973.11), Federal Research Program (IAP 6/18), European Research Program FP6 ApopTrain (MRTN-CT-035624), FP7 Apo-Sys 200767, and the Euregional PACTII. PV holds a Methusalem grant (BOF09/01M00709) from the Flemish Government. MF and JG are supported by Ministry of Science and Higher education grant N N401 037138 European Regional Development Fund through Innovative Economy grant POIG.01.01.02-00-008/08. MF and JG are members of TEAM Programme co-financed by the Foundation for Polish Science and the EU European Regional Development Fund. JG is a recipient of the Mistrz Award from the Foundation for Polish Science. GBF is supported by a postdoctoral fellowship (FWO) and CM is supported by a clinical fellowship (FWO). We thank Jan Piessens (PA's lab), Liesbeth Heyndrickx (PV's lab), Vik Van Duppen (SCIL, Flow cytometry core), and Christine Michiels (WA's lab) for technical support. We acknowledge 'The Hercules Foundation' for supporting access to RNAi collections and associated facilities (grant AUGE/09/040 to PV) and for the Nikon A1R confocal microscope (AKUL/09/037 to WA). Some of the figures were produced using Servier Medical Art (http://www.servier.com), for which the authors would like to acknowledge Servier. Research in Roebroek's group is supported by grants from the KU Leuven (GOA/12/016) and FWO-Vlaanderen (G.0529.08 and G.0689.10). WA is supported by VIB and KU Leuven (GOA/11/009).

*Author contributions:* ADG contributed substantially to the study design, acquisition of most of the data as well as analysis/interpretation of data. Played a major role in drafting of the manuscript. DVK contributed to study design, construction of shRNA constructs, and their stable transduction, acquisition of (mainly *in vivo*) data, analysis of inflammatory profile of APCs and analysis/interpretation of data. Assisted in critical revising of the manuscript. TV contributed to acquisition of *in-vitro* ER stress data and optimization of surface biotinylation protocol. GBF and CM contributed towards isolation and differentiation of hu-iDCs. TM and PW contributed towards *in-vivo* data acquisition and design of *in-vivo* experiments. AK contributed towards the *in-vivo* experiments and mice handling. NR contributed towards microscopic data acquisition and protocols. MF contributed towards acquisition of Photofrin-PDT associated data. AJMR contributed towards making of tools associated with the LRP1/CD91 analysis. WA contributed towards exocytosis/secretory pathway data analysis. JG contributed towards study design and assisted in critical revising of the manuscript. PV contributed towards study design and assisted in critical revising of the manuscript. PA played a substantially major role in conception as well as design of the study, data analysis/interpretation and drafting as well as critical revising of the manuscript.

## Conflict of interest

The authors declare that they have no conflict of interest.

## References

Abe M, Setoguchi Y, Tanaka T, Awano W, Takahashi K, Ueda R, Nakamura A, Goto S (2009) Membrane protein location-dependent regulation by PI3K (III) and rabenosyn-5 in Drosophila wing cells. *PLoS One* **4:** e7306

Agostinis P, Berg K, Cengel KA, Foster TH, Girotti AW, Gollnick SO, Hahn SM, Hamblin MR, Juzeniene A, Kessel D, Korbelik M, Moan J, Mroz P, Nowis D, Piette J, Wilson BC, Golab J (2011) Photodynamic therapy of cancer: an update. *CA Cancer J Clin* **61:** 250–281

Agostinis P, Vantieghem A, Merlevede W, de Witte PA (2002) Hypericin in cancer treatment: more light on the way. *Int J Biochem Cell Biol* **34:** 221–241

Aymeric L, Apetoh L, Ghiringhelli F, Tesniere A, Martins I, Kroemer G, Smyth MJ, Zitvogel L (2010) Tumor cell death and ATP release prime dendritic cells and efficient anticancer immunity. *Cancer Res* **70:** 855–858

Bajor A, Tischer S, Figueiredo C, Wittmann M, Immenschuh S, Blasczyk R, Eiz-Vesper B (2011) Modulatory role of calreticulin as chaperokine for dendritic cell-based immunotherapy. *Clin Exp Immunol* **165:** 220–234

Becker AJ, Uckert S, Tsikas D, Noack H, Stief CG, Frolich JC, Wolf G, Jonas U (2000) Determination of nitric oxide metabolites by means of the Griess assay and gas chromatography-mass spectrometry in the cavernous and systemic blood of healthy males and patients with erectile dysfunction during different functional conditions of the penis. *Urol Res* **28:** 364–369

Bravo R, Vicencio JM, Parra V, Troncoso R, Munoz JP, Bui M, Quiroga C, Rodriguez AE, Verdejo HE, Ferreira J, Iglewski M,

Chiong M, Simmen T, Zorzano A, Hill JA, Rothermel BA, Szabadkai G, Lavandero S (2011) Increased ER-mitochondrial coupling promotes mitochondrial respiration and bioenergetics during early phases of ER stress. *J Cell Sci* **124**(Part 13)**:** 2143–2152

Buytaert E, Callewaert G, Hendrickx N, Scorrano L, Hartmann D, Missiaen L, Vandenheede JR, Heirman I, Grooten J, Agostinis P (2006) Role of endoplasmic reticulum depletion and multidomain proapoptotic BAX and BAK proteins in shaping cell death after hypericin-mediated photodynamic therapy. *FASEB J* **20:** 756–758

Buytaert E, Dewaele M, Agostinis P (2007) Molecular effectors of multiple cell death pathways initiated by photodynamic therapy. *Biochim Biophys Acta* **1776:** 86–107

Buytaert E, Matroule JY, Durinck S, Close P, Kocanova S, Vandenheede JR, de Witte PA, Piette J, Agostinis P (2008) Molecular effectors and modulators of hypericin-mediated cell death in bladder cancer cells. *Oncogene* **27:** 1916–1929

Campos-Toimil M, Bagrij T, Edwardson JM, Thomas P (2002) Two modes of secretion in pancreatic acinar cells: involvement of phosphatidylinositol 3-kinase and regulation by capacitative Ca(2 + ) entry. *Curr Biol* **12:** 211–215

Castano AP, Mroz P, Hamblin MR (2006) Photodynamic therapy and anti-tumour immunity. *Nat Rev Cancer* **6:** 535–545

Chao MP, Jaiswal S, Weissman-Tsukamoto R, Alizadeh AA, Gentles AJ, Volkmer J, Weiskopf K, Willingham SB, Raveh T, Park CY, Majeti R, Weissman IL (2010) Calreticulin is the dominant pro-phagocytic signal on multiple human cancers and is counterbalanced by CD47. *Sci Transl Med* **2:** 63ra94

Chekeni FB, Elliott MR, Sandilos JK, Walk SF, Kinchen JM, Lazarowski ER, Armstrong AJ, Penuela S, Laird DW, Salvesen GS, Isakson BE, Bayliss DA, Ravichandran KS (2010) Pannexin 1 channels mediate 'find-me' signal release and membrane permeability during apoptosis. *Nature* **467:** 863–867

Cousin MA, Malladi CS, Tan TC, Raymond CR, Smillie KJ, Robinson PJ (2003) Synapsin I-associated phosphatidylinositol 3-kinase mediates synaptic vesicle delivery to the readily releasable pool. *J Biol Chem* **278:** 29065–29071

Elliott MR, Chekeni FB, Trampont PC, Lazarowski ER, Kadl A, Walk SF, Park D, Woodson RI, Ostankovich M, Sharma P, Lysiak JJ, Harden TK, Leitinger N, Ravichandran KS (2009) Nucleotides released by apoptotic cells act as a find-me signal to promote phagocytic clearance. *Nature* **461:** 282–286

Ferreira GB, van Etten E, Lage K, Hansen DA, Moreau Y, Workman CT, Waer M, Verstuyf A, Waelkens E, Overbergh L, Mathieu C (2009) Proteome analysis demonstrates profound alterations in human dendritic cell nature by TX527, an analogue of vitamin D. *Proteomics* **9:** 3752–3764

Gardai SJ, McPhillips KA, Frasch SC, Janssen WJ, Starefeldt A, Murphy-Ullrich JE, Bratton DL, Oldenborg PA, Michalak M, Henson PM (2005) Cell-surface calreticulin initiates clearance of viable or apoptotic cells through trans-activation of LRP on the phagocyte. *Cell* **123:** 321–334

Garg AD, Krysko DV, Vandenabeele P, Agostinis P (2011) DAMPs and PDT-mediated photo-oxidative stress: exploring the unknown. *Photochem Photobiol Sci* **10:** 670–680

Garg AD, Nowis D, Golab J, Agostinis P (2010a) Photodynamic therapy: illuminating the road from cell death towards anti-tumour immunity. *Apoptosis* **15:** 1050–1071

Garg AD, Nowis D, Golab J, Vandenabeele P, Krysko DV, Agostinis P (2010b) Immunogenic cell death, DAMPs and anticancer therapeutics: an emerging amalgamation. *Biochim Biophys Acta* **1805:** 53–71

Ghiringhelli F, Apetoh L, Tesniere A, Aymeric L, Ma Y, Ortiz C, Vermaelen K, Panaretakis T, Mignot G, Ullrich E, Perfettini JL, Schlemmer F, Tasdemir E, Uhl M, Genin P, Civas A, Ryffel B, Kanellopoulos J, Tschopp J, Andre F *et al* (2009) Activation of the NLRP3 inflammasome in dendritic cells induces IL-1beta-dependent adaptive immunity against tumors. *Nat Med* **15:** 1170–1178

Gonzalez-Gronow M, Kaczowka SJ, Payne S, Wang F, Gawdi G, Pizzo SV (2007) Plasminogen structural domains exhibit different functions when associated with cell surface GRP78 or the voltage-dependent anion channel. *J Biol Chem* **282:** 32811–32820

Green DR, Ferguson T, Zitvogel L, Kroemer G (2009) Immunogenic and tolerogenic cell death. *Nat Rev Immunol* **9:** 353–363

Gupta S, McGrath B, Cavener DR (2010) PERK (EIF2AK3) regulates proinsulin trafficking and quality control in the secretory pathway. *Diabetes* **59:** 1937–1947

Hendrickx N, Volanti C, Moens U, Seternes OM, de Witte P, Vandenheede JR, Piette J, Agostinis P (2003) Up-regulation of cyclooxygenase-2 and apoptosis resistance by p38 MAPK in hypericin-mediated photodynamic therapy of human cancer cells. *J Biol Chem* **278:** 52231–52239

Jensen LJ, Kuhn M, Stark M, Chaffron S, Creevey C, Muller J, Doerks T, Julien P, Roth A, Simonovic M, Bork P, von Mering C (2009) STRING 8—a global view on proteins and their functional interactions in 630 organisms. *Nucleic Acids Res* **37** (Database issue)**:** D412–D416

Kepp O, Tesniere A, Zitvogel L, Kroemer G (2009) The immunogenicity of tumor cell death. *Curr Opin Oncol* **21:** 71–76

Kim R, Emi M, Tanabe K (2006) Cancer immunosuppression and autoimmune disease: beyond immunosuppressive networks for tumour immunity. *Immunology* **119:** 254–264

Korbelik M, Sun J, Cecic I (2005) Photodynamic therapy-induced cell surface expression and release of heat shock proteins: relevance for tumor response. *Cancer Res* **65:** 1018–1026

Krysko DV, Vandenabeele P (2008) From regulation of dying cell engulfment to development of anti-cancer therapy. *Cell Death Differ* **15:** 29–38

Lancaster GI, Febbraio MA (2005) Exosome-dependent trafficking of HSP70: a novel secretory pathway for cellular stress proteins. *J Biol Chem* **280:** 23349–23355

Laurino L, Wang XX, de la Houssaye BA, Sosa L, Dupraz S, Caceres A, Pfenninger KH, Quiroga S (2005) PI3K activation by IGF-1 is essential for the regulation of membrane expansion at the nerve growth cone. *J Cell Sci* **118**(Part 16)**:** 3653–3662

Locher C, Conforti R, Aymeric L, Ma Y, Yamazaki T, Rusakiewicz S, Tesniere A, Ghiringhelli F, Apetoh L, Morel Y, Girard JP, Kroemer G, Zitvogel L (2010) Desirable cell death during anticancer chemotherapy. *Ann NY Acad Sci* **1209:** 99–108

Low PC, Misaki R, Schroder K, Stanley AC, Sweet MJ, Teasdale RD, Vanhaesebroeck B, Meunier FA, Taguchi T, Stow JL (2010) Phosphoinositide 3-kinase delta regulates membrane fission of Golgi carriers for selective cytokine secretion. *J Cell Biol* **190:** 1053–1065

Luo S, Xing D, Wei Y, Chen Q (2010) Inhibitive effects of photofrin on cellular autophagy. *J Cell Physiol* **224:** 414–422

Martins I, Tesniere A, Kepp O, Michaud M, Schlemmer F, Senovilla L, Seror C, Metivier D, Perfettini JL, Zitvogel L, Kroemer G (2009) Chemotherapy induces ATP release from tumor cells. *Cell Cycle* **8:** 3723–3728

Minotti G, Menna P, Salvatorelli E, Cairo G, Gianni L (2004) Anthracyclines: molecular advances and pharmacologic developments in antitumor activity and cardiotoxicity. *Pharmacol Rev* **56:** 185–229

Nandigama R, Padmasekar M, Wartenberg M, Sauer H (2006) Feed forward cycle of hypotonic stress-induced ATP release, purinergic receptor activation, and growth stimulation of prostate cancer cells. *J Biol Chem* **281:** 5686–5693

Nyasae LK, Hubbard AL, Tuma PL (2003) Transcytotic efflux from early endosomes is dependent on cholesterol and glycosphingolipids in polarized hepatic cells. *Mol Biol Cell* **14:** 2689–2705

Obeid M, Tesniere A, Ghiringhelli F, Fimia GM, Apetoh L, Perfettini JL, Castedo M, Mignot G, Panaretakis T, Casares N, Metivier D, Larochette N, van Endert P, Ciccosanti F, Piacentini M, Zitvogel L, Kroemer G (2007) Calreticulin exposure dictates the immunogenicity of cancer cell death. *Nat Med* **13:** 54–61

Panaretakis T, Joza N, Modjtahedi N, Tesniere A, Vitale I, Durchschlag M, Fimia GM, Kepp O, Piacentini M, Froehlich KU, van Endert P, Zitvogel L, Madeo F, Kroemer G (2008) The co-translocation of ERp57 and calreticulin determines the immunogenicity of cell death. *Cell Death Differ* **15:** 1499–1509

Panaretakis T, Kepp O, Brockmeier U, Tesniere A, Bjorklund AC, Chapman DC, Durchschlag M, Joza N, Pierron G, van Endert P, Yuan J, Zitvogel L, Madeo F, Williams DB, Kroemer G (2009) Mechanisms of pre-apoptotic calreticulin exposure in immunogenic cell death. *EMBO J* **28:** 578–590

Patel JM, Li YD, Zhang J, Gelband CH, Raizada MK, Block ER (1999) Increased expression of calreticulin is linked to ANG IV-mediated activation of lung endothelial NOS. *Am J Physiol* **277**(4 Part 1)**:** L794–L801

Peters LR, Raghavan M (2011) Endoplasmic reticulum calcium depletion impacts chaperone secretion, innate immunity, and phagocytic uptake of cells. *J Immunol* **187:** 919–931

 

Reekmans SM, Pflanzner T, Gordts PL, Isbert S, Zimmermann P, Annaert W, Weggen S, Roebroek AJ, Pietrzik CU (2010) Inactivation of the proximal NPXY motif impairs early steps in LRP1 biosynthesis. *Cell Mol Life Sci* **67:** 135–145

Rodriguez JA, Span SW, Kruyt FA, Giaccone G (2003) Subcellular localization of CrmA: identification of a novel leucine-rich nuclear export signal conserved in anti-apoptotic serpins. *Biochem J* **373**(Part 1)**:** 251–259

Roebroek AJ, Reekmans S, Lauwers A, Feyaerts N, Smeijers L, Hartmann D (2006) Mutant Lrp1 knock-in mice generated by recombinase-mediated cassette exchange reveal differential importance of the NPXY motifs in the intracellular domain of LRP1 for normal fetal development. *Mol Cell Biol* **26:** 605–616

Safaei R, Katano K, Larson BJ, Samimi G, Holzer AK, Naerdemann W, Tomioka M, Goodman M, Howell SB (2005) Intracellular localization and trafficking of fluorescein-labeled cisplatin in human ovarian carcinoma cells. *Clin Cancer Res* **11**(2 Part 1)**:** 756–767

Scorrano L, Oakes SA, Opferman JT, Cheng EH, Sorcinelli MD, Pozzan T, Korsmeyer SJ (2003) BAX and BAK regulation of endoplasmic reticulum Ca2 + : a control point for apoptosis. *Science* **300:** 135–139

Spisek R, Charalambous A, Mazumder A, Vesole DH, Jagannath S, Dhodapkar MV (2007) Bortezomib enhances dendritic cell (DC)-mediated induction of immunity to human myeloma via exposure of cell surface heat shock protein 90 on dying tumor cells: therapeutic implications. *Blood* **109:** 4839–4845

Stafford JL, Galvez F, Goss GG, Belosevic M (2002) Induction of nitric oxide and respiratory burst response in activated goldfish macrophages requires potassium channel activity. *Dev Comp Immunol* **26:** 445–459

Szokalska A, Makowski M, Nowis D, Wilczynski GM, Kujawa M, Wojcik C, Mlynarczuk-Bialy I, Salwa P, Bil J, Janowska S, Agostinis P, Verfaillie T, Bugajski M, Gietka J, Issat T, Glodkowska E, Mrowka P, Stoklosa T, Hamblin MR, Mroz P *et al* (2009) Proteasome inhibition potentiates antitumor effects of photodynamic therapy in mice through induction of endoplasmic reticulum stress and unfolded protein response. *Cancer Res* **69:** 4235–4243

Teske BF, Wek SA, Bunpo P, Cundiff JK, McClintick JN, Anthony TG, Wek RC (2011) The eIF2 kinase PERK and the integrated stress response facilitate activation of ATF6 during endoplasmic reticulum stress. *Mol Biol Cell* **22:** 4390–4405

Tufi R, Panaretakis T, Bianchi K, Criollo A, Fazi B, Di Sano F, Tesniere A, Kepp O, Paterlini-Brechot P, Zitvogel L, Piacentini M, Szabadkai G, Kroemer G (2008) Reduction of endoplasmic reticulum Ca2 + levels favors plasma membrane surface exposure of calreticulin. *Cell Death Differ* **15:** 274–282

Vantieghem A, Assefa Z, Vandenabeele P, Declercq W, Courtois S, Vandenheede JR, Merlevede W, de Witte P, Agostinis P (1998) Hypericin-induced photosensitization of HeLa cells leads to apoptosis or necrosis. Involvement of cytochrome c and procaspase-3 activation in the mechanism of apoptosis. *FEBS Lett* **440:** 19–24

Vergely C, Delemasure S, Cottin Y, Rochette L (2007) Preventing the cardiotoxic effects of anthracyclines: from basic concepts to clinical data. *Heart Metab* **35:** 1–7

Wang HT, Lee HI, Guo JH, Chen SH, Liao ZK, Huang KW, Torng PL, Hwang LH (2011a) Calreticulin promotes tumor lymphocyte infiltration and enhances the antitumor effects of immunotherapy by up-regulating the endothelial expression of adhesion molecules. *Int J Cancer* (10.1002/ijc.26339)

Wang X, Olberding KE, White C, Li C (2011b) Bcl-2 proteins regulate ER membrane permeability to luminal proteins during ER stress-induced apoptosis. *Cell Death Differ* **18:** 38–47

Willnow TE, Herz J (1994) Genetic deficiency in low density lipoprotein receptor-related protein confers cellular resistance to Pseudomonas exotoxin A. Evidence that this protein is required for uptake and degradation of multiple ligands. *J Cell Sci* **107**(Part 3)**:** 719–726

Wilson ML, Guild SB (2001) Effects of wortmannin upon the late stages of the secretory pathway of AtT-20 cells. *Eur J Pharmacol* **413:** 55–62

Yuan TL, Cantley LC (2008) PI3K pathway alterations in cancer: variations on a theme. *Oncogene* **27:** 5497–5510

Zai A, Rudd MA, Scribner AW, Loscalzo J (1999) Cell-surface protein disulfide isomerase catalyzes transnitrosation and regulates intracellular transfer of nitric oxide. *J Clin Invest* **103:** 393–399

Zamaraeva MV, Sabirov RZ, Maeno E, Ando-Akatsuka Y, Bessonova SV, Okada Y (2005) Cells die with increased cytosolic ATP during apoptosis: a bioluminescence study with intracellular luciferase. *Cell Death Differ* **12:** 1390–1397

Zhang Y, Liu R, Ni M, Gill P, Lee AS (2010) Cell surface relocalization of the endoplasmic reticulum chaperone and unfolded protein response regulator GRP78/BiP. *J Biol Chem* **285:** 15065–15075

Zitvogel L, Kepp O, Kroemer G (2010a) Decoding cell death signals in inflammation and immunity. *Cell* **140:** 798–804

Zitvogel L, Kepp O, Senovilla L, Menger L, Chaput N, Kroemer G (2010b) Immunogenic tumor cell death for optimal anticancer therapy: the calreticulin exposure pathway. *Clin Cancer Res* **16:** 3100–3104

Zitvogel L, Tesniere A, Kroemer G (2006) Cancer despite immunosurveillance: immunoselection and immunosubversion. *Nat Rev Immunol* **6:** 715–727